Radioisotope Geochronology of Lake Superior Sediments

BY

COLIN COOK SMALLEY
B.S.Evs., Creighton University, 2010

THESIS

Submitted as partial fulfillment of the requirements
for the degree of Master of Science in Earth and Environmental Sciences
in the Graduate College of the
University of Illinois at Chicago, 2013

Chicago, Illinois

Defense Committee:
Neil Sturchio, Chair and Advisor
Peter Doran
Barry Lesht

This thesis is dedicated to my spouse, Elsbeth, whose support never wavered throughout my graduate studies.

ACKNOWLEDGEMENTS

I would like to thank my thesis committee – Neil Sturchio, Peter Doran, and Barry Lesht. Their support and comments have been invaluable in accomplishing my research and academic goals here at the University of Illinois at Chicago. I would also like to acknowledge the constant support and encouragement of Meg Corcoran, my office mate, colleague, and trailblazer in this program.

I owe a great deal of thanks as well to the rest of the team of researchers involved with the Great Lakes Sediment Surveillance Project – Principal Investigator An Li, Co-PI Karl Rockne – and graduate student colleagues Jiehong Guo, Solidea Maria Christina Bonina, and Soheil Hosseini. It has been a pleasure working in the field and in the lab with you all. Furthermore I need to acknowledge the captain and crew of the R/V *Lake Guardian* and other UIC researchers including Gregory Bourgon, Felipe Tendick-Matesanz, and Andy Sandy for their outstanding work in collecting the Lake Superior samples. Thanks also go to Cindy Craig at the National Geodetic Survey for NADCON assistance.

Finally, I would like to thank the U.S. Environmental Protection Agency, who funds the GLSSP program, as well as UIC Chancellor Paula Allen-Meares, for her support in the form of a Chancellor's Graduate Research Fellowship. I also would like to thank Steve Forman for helpful conversations, as well as his unwavering support throughout my experience in this department.

CCS

TABLE OF CONTENTS

LIST OF FIGURES

FIGURE PAGE

LIST OF TABLES

SUMMARY

A geochronologic study was carried out on nine sediment cores obtained from Lake Superior in 2011. Activity profiles of four radioactive isotopes of lead, radium, cesium, and americium were obtained for each core using gamma spectroscopy. Calculations of the sedimentation rate, focusing factor, and absolute dates were performed where possible. These results were combined with results from previous studies in Lake Superior to create an updated map of sedimentation rates in Lake Superior – the first update to the original map published over 30 years ago.

Sedimentation rates were obtained for eight cores, and absolute dates were obtained for six of those. Two of these cores provide data in parts of the lake that have not been previously studied: the basin to the northeast of Isle Royale, and the northeast side of the Duluth sub-basin. Results in these areas provide new evidence for previously-established lake circulation and sediment transport models. All sedimentation rates were within the range of previously-reported values for Lake Superior, with the highest occurring near Duluth, Minnesota, and the lowest occurring in the highly complex Caribou sub-basin area.

1. Introduction

Despite Lake Superior being the largest freshwater lake in the world by surface area, comprehensive studies of Lake Superior sedimentation rates are rare. Only four studies (Kemp et al. 1978, Evans et al. 1981, Klump et al. 1989, Song et al. 2004) have determined sedimentation rates and focusing factors for three or more of the ten depositional areas identified by Thomas and Dell (1978). This project determines sedimentation characteristics in five of these ten depositional areas, which has not been done by any single study since Evans et al. (1981). Sediment has been found to have differences in accumulation and transport behavior throughout the lake, and this project increases the spatial resolution of our understanding of this complex system.

The sediments of the Great Lakes are important archives having potential to help understand several major environmental questions, including the mechanics of sediment movement and accumulation, trends in anthropogenic pollution, and evidence of major storm events over the last 200 years or more.

The objectives of this study are:

(1) Provide the time constraints necessary to quantify in the depositional history of pollutants including chlorinated and brominated compounds, perfluorinated compounds (PFCs), and pharmaceuticals and personal care products (PPCPs) measured in the same sediment core profiles.

(2) Evaluate the evidence for sediment mixing from discrete events such as major storms in 1905, 1918, and 1950 as well as ongoing processes such as bioturbation, and

(3) Compare results from this project to previous geochronological efforts in Lake Superior, including an analysis of basin-scale sedimentation patterns.

2. Background

2.1. Previously-Utilized Geochronology Methods

Geochronology of sediment cores in Lake Superior has been studied by measuring concentrations of various pollen grains, and by analysis of the activities of ^{210}Pb and ^{137}Cs. Each geochronologic method has certain strengths, and where possible, past efforts have involved multiple methods as a "check" on the primary method (Bruland et al. 1975, Klump et al. 1989, Appleby 2001).

Many of the earliest geochronologies of Lake Superior sediments were performed by pollen analysis. In Lake Superior studies, this method relies on the pollen of the *Ambrosia* genus (ragweed) and sometimes *Pinus* (pine) as well (Bruland et al. 1975, Kemp et al. 1978). The areas upwind from Lake Superior were cleared of forest to allow for agriculture, and the wind-carried pollen signatures changed accordingly. By comparison with a nearby sample that is easily dated, such as varved sediments, a time horizon for the onset of *Ambrosia* or a decline in *Pinus* may be obtained and used for dating lake cores (Robbins et al. 1978).

Subsequent studies of Lake Superior sediments have utilized ^{137}Cs as a time horizon in a similar manner to pollen, which is to determine an onset date and a peak date. Because ^{137}Cs is not naturally occurring, and was introduced due to detonations of nuclear weapons, the dates of onset and peak of atmospheric ^{137}Cs are well constrained. The first such detonations occurred in 1952, with fallout of the ^{137}Cs occurring in North America starting in 1954 (Appleby 2001). The peak

activity of ^{137}Cs occurred in 1963-1964, immediately before the Limited Test Ban Treaty which significantly reduced the number of nuclear weapon detonations worldwide (Appleby 2001).

Finally, the most common geochronology method for Lake Superior sediments utilizes ^{210}Pb activities. With a half-life of 22.3 years, ^{210}Pb is widely used for dating recently-deposited sediments, in general within the last 150 years (Appleby 2001). The ^{210}Pb method requires knowledge first of whether or not the general trend in sediment accumulation is constant. Once that has been determined, knowledge of the annual flux of atmospheric ^{210}Pb allows for use of one of several models to determine dates throughout the core.

2.2. Lead-210 in Sediment: Sources and Processes

^{210}Pb is a naturally-occurring radioisotope which is part of the ^{238}U decay series. When ^{226}Ra decays to ^{222}Rn, which is a gas, fractionation occurs as some amount of radon gas escapes the sediment matrix and is exhaled to the atmosphere. The ^{222}Rn that cannot escape decays with a 3.8-day half-life *in situ* through several short-lived daughter nuclides to ^{210}Pb, which is known as supported lead. The parent nuclides of ^{210}Pb are also naturally-occurring, and ^{238}U (half-life of 4.6×10^9 years) is present in the sediments underlying the lake as well as sediments that have been transported to the lake by fluvial or other processes. The supported ^{210}Pb is generally near equilibrium with ^{226}Ra, and accordingly, ^{226}Ra activity is sometimes used to determine the amount of supported ^{210}Pb in a sample.

2.3. Excess Lead-210

The remainder of the ^{210}Pb in the sediments of Lake Superior comes from atmospheric deposition of ^{210}Pb produced by decay of atmospheric ^{222}Rn. This is known as the unsupported or excess ^{210}Pb. Because ^{222}Rn has a sufficiently long half-life of 3.8 days, it is transported through the troposphere and can even reach the stratosphere at times (Robbins 1978). Therefore, over time the influx of unsupported ^{210}Pb, especially over an area as large as Lake Superior, is often assumed to be constant (e.g. Robbins and Edgington 1975). This influx is primarily due to the fact that ^{210}Pb is easily scavenged by atmospheric aerosols and returns to the surface with snow, rain, and dry fallout. This ^{210}Pb that falls over the lake surface attaches to particles, travels through the water column, and is deposited with the bottom sediments.

2.4. Cesium-137 in Sediment: Sources and Processes

With the advent of large-yield nuclear weapons testing, radioactive debris particles entered the stratosphere and dispersed globally. Eventually, these particles reentered the troposphere and fallout of isotopes including ^{137}Cs and ^{241}Am reached the surface of land or water. The amount of fallout varied spatially with factors such as precipitation and latitude, and varied temporally with the occurrence of above-ground nuclear weapon detonations. These detonations were constrained by two major political events: the signing of a moratorium in 1958 that lasted until 1961, and a more permanent, but less far-reaching Limited Test Ban Treaty that was signed in 1963. Between these two events, a sharp increase in

testing occurred, creating a distinctive peak in 1963-1964 (Appleby 2001). Despite spatial variations of fallout in Lake Superior, it is expected that the temporal variation signal of fallout isotopes remains a significant marker in Lake Superior sediments.

2.5. Lake Superior Size

Lake Superior is one of the largest lakes in the world: it is the largest freshwater lake by surface area, and the third-largest by volume, behind Lake Baikal and Lake Tanganyika. With a volume of 12,115 km^3 and a surface area of 82,100 km^2, Lake Superior has a water residence time of 173 years, making it the slowest of the Great lakes to respond to contaminant loading (Quinn 1992). The maximum depth in Lake Superior is generally regarded as 405 m (e.g., Munawar 1978); however, Klump et al. (1989) reported a sample depth of 410m in their 1986 survey.

2.6. Lake Superior Basin Characteristics

The area of the Lake Superior Basin watershed is approximately 125,000 km^2, not including Lake Superior itself (see

Figure **1** for a basin map). Of this, approximately 73% is forest land, 10% is open water, and only 1.75% is land developed by humans (Hollenhorst et al. 2011).

Runoff from the Lake Superior Basin, which was 60.75 cm/year on average from 1948-1999, accounts for approximately 43% of all water input into Lake Superior (Lenters 2004). The runoff is derived from several major rivers, as well as smaller drainages around the lake. The largest river in terms of input to Lake

Superior is the Iron River of Michigan, which has the smallest watershed of the major rivers (Bennett 1978). Similarly, the river with the largest drainage area is the St. Louis River with a mouth near Duluth, Minnesota, and it has the lowest discharge to Lake Superior (Bennett 1978).

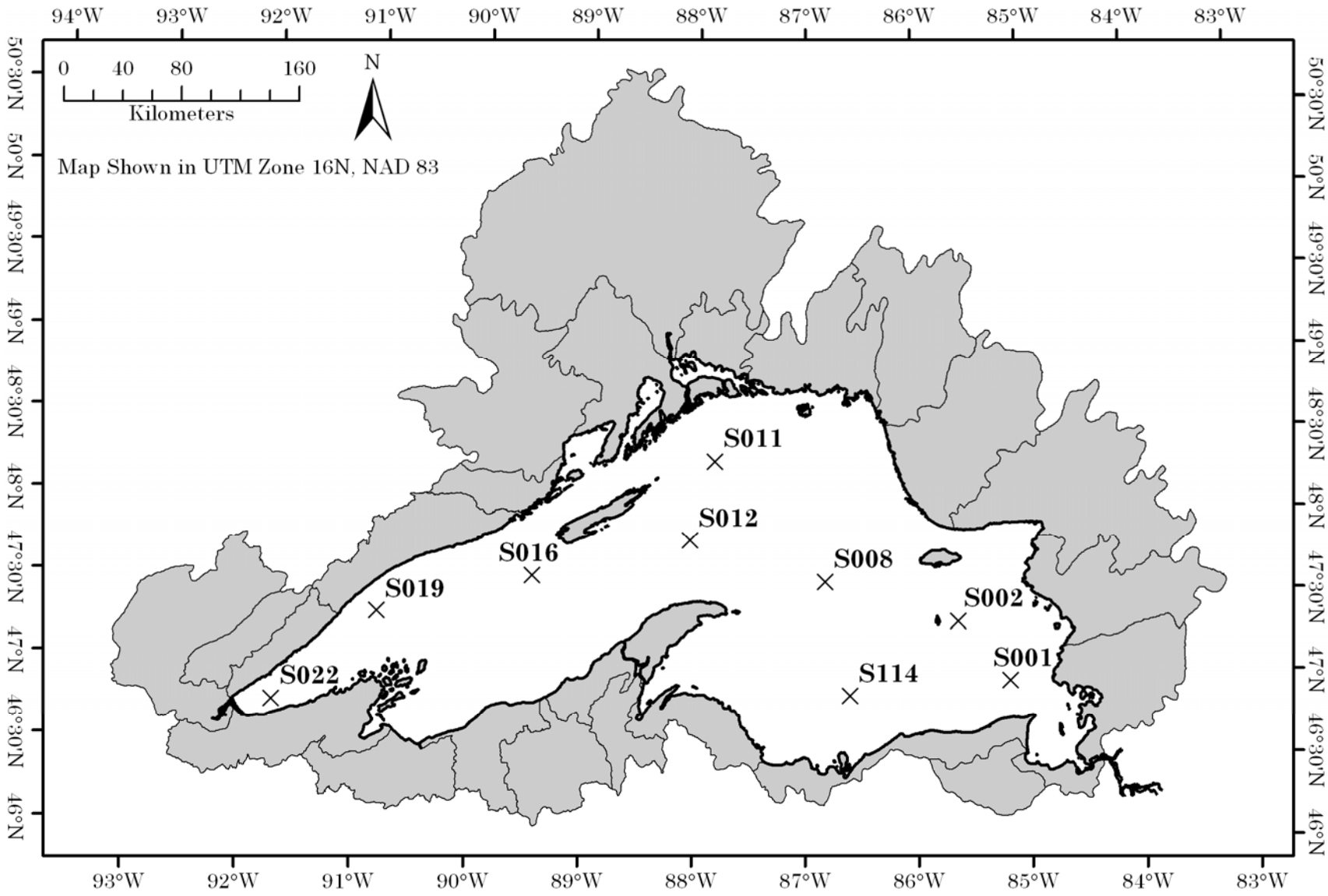

Figure 1. Drainage basins of the Lake Superior watershed. Sample locations (this study) shown for reference.

2.7. Lake Superior Bathymetry

The bathymetry of Lake Superior has generally been categorized into two main sections, with large abyssal plains in the western half of the lake, and a much more complex bathymetry east of the Keweenaw Peninsula (Klump et al. 1989). In the eastern half of the lake, the bathymetry is described as having steep relief, north-south troughs, and deep basins (Klump et al. 1989). The complexity of the eastern basins is attributed to a combination of glacial outwash and the effects of lake currents in the last 7,000 years (Flood & Johnson 1984).

However, several studies (Flood and Johnson 1984, Cartwright et al. 2004, Johnson et al. 2012) have documented the presence of ring-shaped depressions 100 to 400 m in diameter and 1 to 7 m deep in the western basins of Lake Superior, suggesting that previous descriptions oversimplified the small-scale topography in the western part of the lake. These small-scale variations are generally attributed to nontectonic faulting due to the dewatering of the clay sediments in this part of the lake (Flood and Johnson 1984).

2.8. Lake Superior Circulation

Understanding lake currents is important to study of sedimentation processes in Lake Superior. Flood and Johnson (1984) describe evidence such as sedimentary furrows and sand ribbons indicating that sediment is transported by currents, at least in the eastern basins of the lake. In a model of Lake Superior circulation, Bennington et al. (2010) determined that circulation is primarily cyclonic in all seasons. In the winter, coastal currents are weaker than in the

summer, and the overall circulation regime consists of two distinct circulation cells (Bennington et al. 2010). In the summer, subsurface flows tend to follow the isobaths of the lake, also setting up a two-cell cyclonic circulation, with strong currents near-shore (Bennington et al. 2010).

2.9. Previous Studies: Analysis of Lake-Wide Sedimentation Patterns

Previous attempts to describe sedimentation patterns in all or part of Lake Superior are found in Kemp et al. (1978), Evans et al. (1981), Klump et al. (1989), and Jeremiason (1993). In general, the consensus is that sedimentation rates are highest on the edges of depositional basins, and in near-shore areas with large influxes of sediment from shoreline erosion or fluvial processes. The lowest rates are found in areas described as flat, relatively shallow off-shore areas and in some basins isolated from sediment sources. Finally, the patterns in the eastern part of the lake are cited as highly complex and potentially unpredictable. This study seeks to test these long-standing conclusions about sedimentation patterns in Lake Superior.

2.10. Previous Studies: Individual Samples

Several previous efforts have dated sediments from Lake Superior, primarily using pollen, alpha spectroscopy, and gamma spectroscopy. The previous efforts are documented in articles which are focused on many topics, but in general such efforts were undertaken to understand better the fate of chemical contaminants in Lake Superior sediments. Sedimentation rates, along with location, depth, sample date, and dating method have been summarized in Table I. Maps showing the location of

the previous samples are presented in Figure 2 and Figure 3. Sedimentation rates have been reported at a total of 70 sites throughout the previous 40 years; however, only 64 of the sites have sedimentation rates reported in units that account for sediment density, such as $g/cm^2/yr$. The range of reported sedimentation rate values is 0.002 – 0.304 $g/cm^2/yr$.

TABLE I. PREVIOUSLY DATED CORES IN LAKE SUPERIOR

Source	Core ID	Measured Depth (m)	Date Sampled	Method	Sedimentation Rate (g/cm²/yr)	Latitude* (degrees)	Longitude* (degrees)	Precision** (degrees)
Maher 1977	71-1397	69	9/23/1971	Pollen		47.0283	-90.9652	± 0.0017
	72-1	265	5/19/1972			47.1516	-91.3335	± 0.0017
	73-20	101	5/23/1973			46.8799	-91.7668	± 0.0017
	73-23	101	5/23/1973			46.8799	-91.7668	± 0.0017
	73-26	26	5/29/1973			47.0783	-91.5468	± 0.0017
Bruland et al. 1975 and Maher 1977	72-240	61	8/18/1972	Pollen and Pb-210 alpha		47.0283	-90.9652	± 0.0017
	72-247	139	9/11/1972			47.4666	-90.0001	± 0.0017
Kemp et al. 1978	25A	201	1973	Pollen	0.0155	48.4499	-87.4984	± 0.0003
	28	242	1973		0.0050	48.0149	-87.6334	± 0.0003
	C-59A	123	1973		0.0700	46.7150	-84.7867	± 0.0003
	G-18	206	1973		0.0050	47.0549	-89.7701	± 0.0003
	H-56A	209	1973		0.0250	47.1883	-85.1168	± 0.0003
	I-7 (0-1cm)	279	1973		0.0340	47.1833	-91.2285	± 0.0003
	I-7 (10-11cm)	279	1973		0.0780	47.1833	-91.2285	± 0.0003
	K.B.	152	1973		0.0435	46.9966	-88.2018	± 0.0003
	L-142	313	1973		0.0025	47.5416	-87.0001	± 0.0003
	S-24	285	1973		0.0460	48.1549	-89.0251	± 0.0003
	T-46A	251	1973		0.0255	48.2916	-86.4168	± 0.0003
Evans et al. 1981 and Evans 1980	C-79 12BX	115	7/01/1979	Pb-210 alpha	0.016	46.8416	-90.2685	± 0.0017
	C-79 14BX	245	7/01/1979		0.015	47.6232	-88.0918	± 0.0017
	C-79 15BX	265	7/02/1979		0.027	48.1882	-88.1884	± 0.0017
	C-79 20BX	136	7/03/1979		0.160	48.7216	-86.4818	± 0.0017
	C-79 23BX	203	7/04/1979		0.014	47.6483	-85.6301	± 0.0017
	C-79 26BX	200	7/04/1979		0.033	47.8733	-85.0001	± 0.0017
	C-79 29BX	143	7/05/1979		0.014	47.3317	-85.4168	± 0.0017
	S-78 11BX	184	7/22/1978		0.010	47.5799	-89.6501	± 0.0017
	S-78 13BX	77	7/23/1978		0.053	48.4065	-88.9451	± 0.0017
	S-78 15BX	186	7/23/1978		0.024	48.3115	-88.5367	± 0.0017
	S-78 1BX	48	7/20/1978		0.045	46.8099	-91.7335	± 0.0017
	S-78 21BX	201	7/25/1978		0.007	48.2049	-88.1034	± 0.0017
	S-78 24BX	175	7/25/1978		0.007	47.8032	-88.4001	± 0.0017
	S-78 26BX	180	7/26/1978		0.022	47.6166	-88.1451	± 0.0017
	S-78 4BX	140	7/21/1978		0.016	47.0533	-91.0702	± 0.0017
	S-78 8BX	86	7/21/1978		0.022	47.2832	-90.6835	± 0.0017
	W-77 11BX	130	7/13/1977		0.069	46.7367	-84.8001	± 0.0017

* All coordinates converted to WGS 1984 Coordinate System. ** Spatial uncertainty due to precision of originally-reported coordinates.

TABLE I. PREVIOUSLY DATED CORES IN LAKE SUPERIOR, CONTINUED

Source	Core ID	Measured Depth (m)	Date Sampled	Method	Sedimentation Rate (g/cm²/yr)	Latitude* (degrees)	Longitude* (degrees)	Precision** (degrees)
Klump et al. 1989	1369	410	1986	Pb-210 alpha and	N. R.	46.8999	-86.6018	± 0.0017
	1373	295	1986	Cs-137 gamma	N. R.	47.2016	-86.0802	± 0.0017
	1377	323	1986		0.055	47.0033	-86.0585	± 0.0017
	1A	152	1985		N. R.	47.3533	-88.6501	± 0.0017
	2	170	1985		N. R.	47.3883	-88.6334	± 0.0017
	3	230	1985		0.018	47.4516	-88.6001	± 0.0017
	CIRB1	212	1985		0.013	47.8382	-88.5268	± 0.0017
	CIRB2	308	1985		0.018	47.9332	-88.1668	± 0.0017
	DHC	410	1985		<< 0.030	46.8999	-86.6018	± 0.0017
	EB	323	1985		0.040	47.2066	-86.0752	± 0.0017
	HB	30	1985		0.080	46.9167	-84.4700	± 0.0017
	IP	132	1985		0.060	46.6834	-84.7834	± 0.0017
	KB1	137	1985		N. R.	47.0833	-87.9668	± 0.0017
	KB2	135	1985		0.019	47.0832	-87.6168	± 0.0017
	SIRB2	269	1985		0.011	47.5416	-88.5668	± 0.0017
Kolak et al. 1998	1383	270	8/03/1986	Pb-210 alpha	0.003 – 0.039	47.6574	-87.9591	± 0.0002
	1391	60	8/03/1986		0.002 – 0.025	46.7570	-84.7844	± 0.0002
Jeremiason 1993	DTL	68.3	8/30/1990	Pb-210 alpha	0.034	46.8507	-91.7632	± 0.0002
and Simcik et al.	NOAA 3	178	8/26/1990		0.012	47.3307	-89.2492	± 0.0002
2003	SJE II	167.3	8/31/1990		0.027	47.0333	-91.2990	± 0.0002
Pearson et al. 1997	Basswood	N.R.	1991	Pb-210 alpha	0.057	47.0833	-90.6667	± 0.0167
Song et al. 2004	SU-08B	302	5/02/2002	Pb-210 alpha	0.0132 – 0.0151	47.6058	-86.8158	± 0.0003
	SU-12	237.5	5/01/2002		0.0121 – 0.0133	47.8561	-88.0419	± 0.0003
	SU-16	181.5	5/01/2002		0.0108 – 0.0111	47.6214	-89.4630	± 0.0003
	SU-22	55.5	4/30/2002		0.0210 – 0.0213	46.8014	-91.7497	± 0.0003
Muir et al. 2009	Superior	N. R.	2001	Pb-210 alpha	0.014	46.9000	-86.5000	± 0.1000
Johnson et al. 2012	BH05-10	201	2005	Pb-210 alpha	0.00673 – 0.00897	47.3512	-89.4741	± 0.0000
	BH05-11	199.5	2005		0.00987	47.3503	-89.4829	± 0.0000
	BH05-2	202	2005		0.00493	47.3567	-89.4849	± 0.0000
	BH05-3	199	2005		0.00807	47.3559	-89.4849	± 0.0000
	BH05-4	200	2005		0.012	47.3555	-89.4827	± 0.0000
	BH05-5	198	2005		0.009 – 0.01794	47.3552	-89.4805	± 0.0000
	BH05-6	202	2005		0.0063 – 0.0166	47.3549	-89.4703	± 0.0000
	BH05-7	200	2005		0.0071	47.3555	-89.4705	± 0.0000
	BH05-8	198	2005		0.00673 – 0.0166	47.3574	-89.4692	± 0.0000
	BH05-9	200	2005		0.00897	47.3545	-89.4691	± 0.0000

* All coordinates converted to WGS 1984 Coordinate System. ** Spatial uncertainty due to precision of originally-reported coordinates.

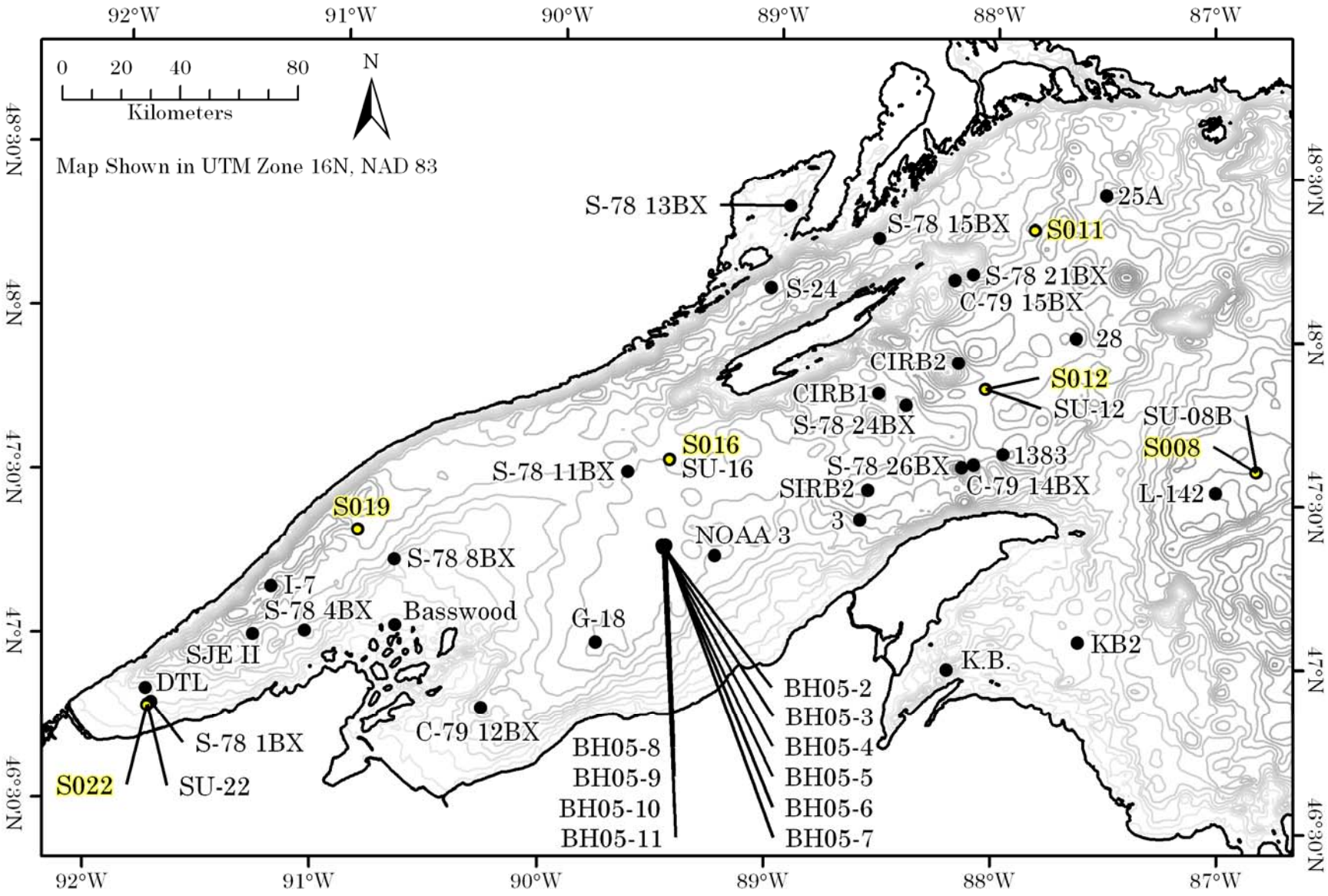

Figure 2. Sediment Core Locations in Western Lake Superior

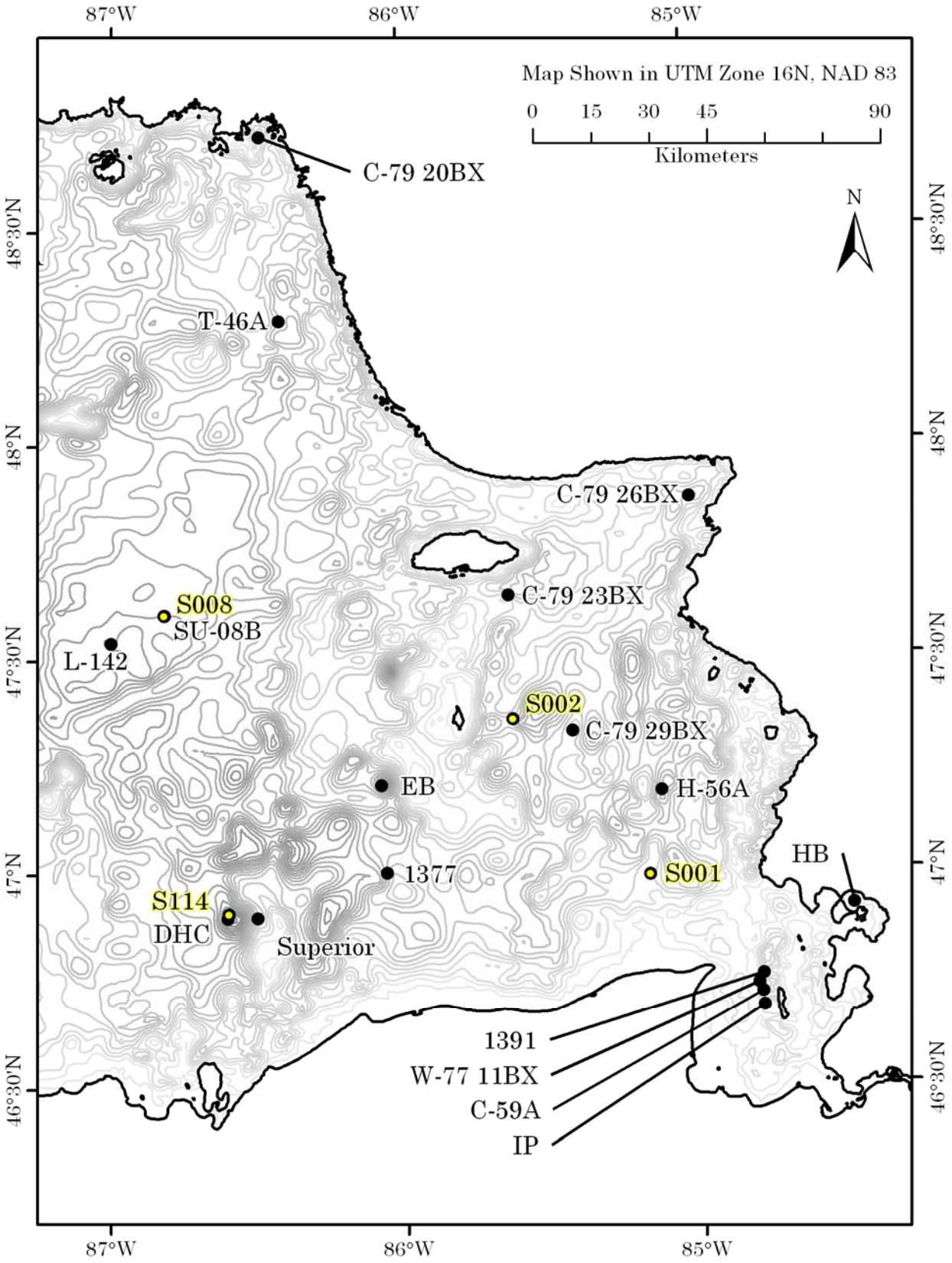

Figure 3. Sediment Core Locations in Eastern Lake Superior

3. Methods

Sample Collection

Sediment sampling on Lake Superior was conducted from May 25th to 29th, 2011, onboard the United States Environmental Protection Agency's research vessel *Lake Guardian*. A total of nine locations were sampled (Table II). Sample locations were U.S. EPA's standard research locations (all except S114). The sample locations were chosen to represent near-shore and open water depositional areas across the entire lake. Spatial data were collected using a Trimble NT200D differential GPS system. Depth data were collected using a Furuno FE 881-MK2 depth sounder, and depths in Table II are adjusted by multiplying by 0.972 to account for operation in freshwater.

TABLE II. SAMPLE LOCATIONS

Location	Date	Time CDT	Latitude (Deg) (1)	Longitude (Deg) (1)	Depth (m)	Core Segments
S001	5/25/2011	04:49	46.9930	-85.1612	95.4	24
S002	5/25/2011	08:31	47.3603	-85.6208	153.7	25
S008	5/25/2011	16:08	47.6058	-86.8177	300.7	25
S019	5/26/2011	17:47	47.3703	-90.8535	187.8	25
S022	5/26/2011	23:43	46.8002	-91.7508	54.5	25
S016	5/27/2011	12:58	47.6212	-89.4633	180.0	25
S012	5/27/2011	21:52	47.8553	-88.0418	238.4	26
S011	5/28/2011	03:38	48.3438	-87.8250	229.6	25
S114	5/29/2011	17:56	46.9095	-86.5980	398.0	26

(1) Latitude and Longitude data are in the WGS 84 coordinate system.

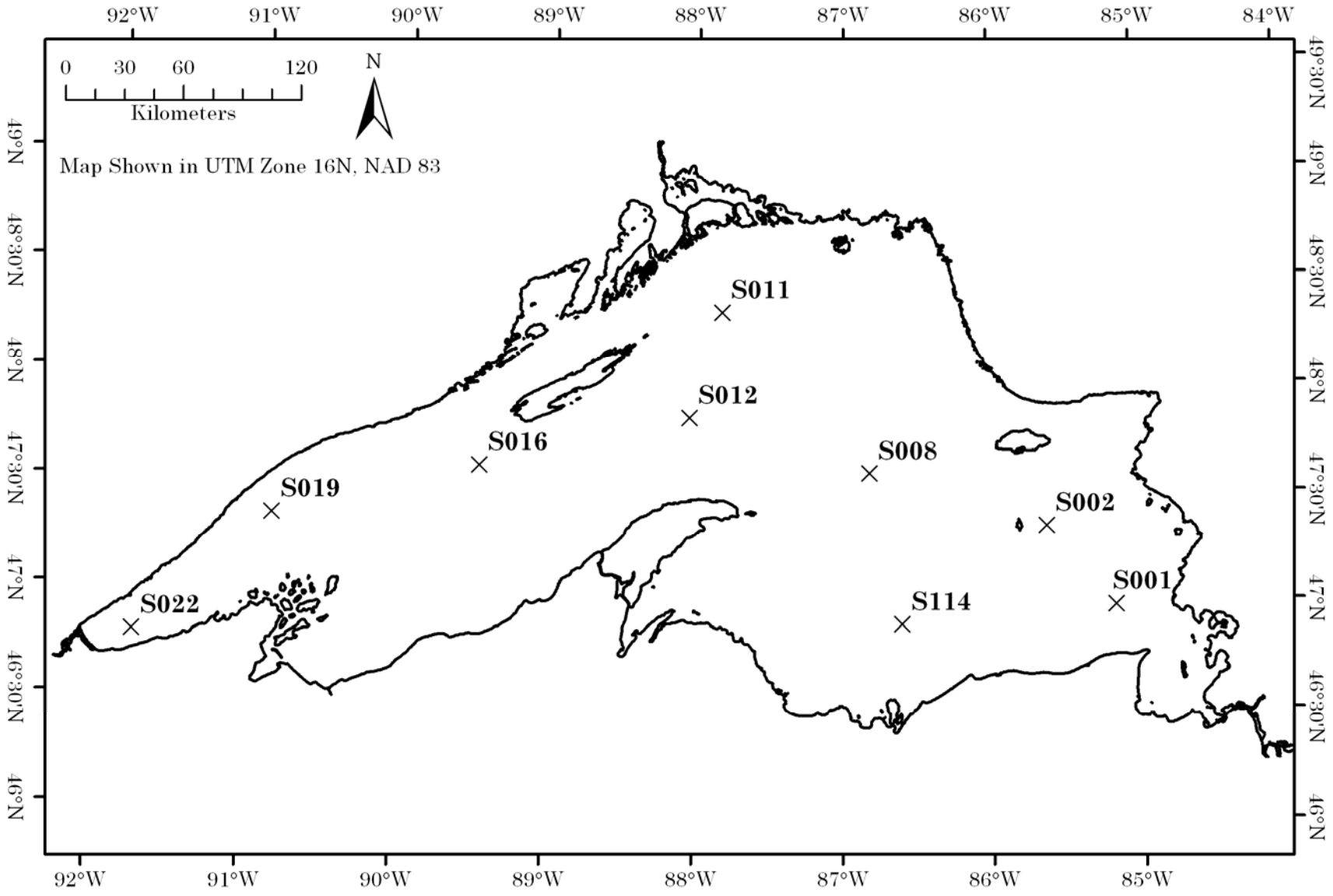

Figure 4. Sediment Core locations for all GLSSP sites (this study).

Samples were collected using a MC-400 Hedrick/Marrs Multi-Corer (Ocean Instruments, San Diego, CA). At each location, the multi-corer was deployed twice to collect bulk sediment with an undisturbed (or minimally-disturbed) sediment-water interface. The multi-corer is capable of recovering four cores per deployment; therefore, a total of eight cores per location were collected.

The cores were collected in polycarbonate tubes with an inner diameter of 9.5cm, an outer diameter of 10cm, and a length of 59.6cm. After each deployment, the bottom end of each tube was closed by hand-inserting a polyethylene puck with double o-rings, before the ends were exposed to air. Care was taken to maintain the vertical position of the cores during the entire process. Each core was then carefully removed from the multi-corer and taken to the general laboratory on the *R/V Lake Guardian* for sectioning.

Each core was extruded, using one of two hydraulic extruders (Cambron Engineering, Bay City, MI). Sectioning was performed according to the following scheme:

- 0.5 cm intervals for the first 5 cm (0cm to 5cm segment depth),
- 1 cm intervals for the next 10 cm (5cm to 15cm segment depth),
- 2 cm intervals for the remainder of the core (15cm to 25cm segment depth).
- At site S012, a deep segment (40-42cm segment depth) was collected from 2 separate cores.
- At site S114, a deep segment (40-42cm segment depth) was collected.

After each section was removed, the sediment segments from each core at corresponding depth were composited in glass bowls. Once all of the cores had been completely extruded, the segments were well mixed with stainless steel spoons. An exception to the process was at site S114, where only segments from the first cast (four cores) were homogenized. All sectioning equipment was thoroughly cleaned using tap water, acetone, and deionized water between each segment.

The samples from each core were placed in the onboard freezer at -20°C until the conclusion of the trip, and were then transported back to the laboratory at the University of Illinois at Chicago in coolers. Upon arrival at UIC, samples were stored in a walk-in freezer at the temperature of -20°C, which was monitored and recorded daily.

3.1. Freeze Drying

Each sample for dating purposes is a sub-sample of the samples collected for use by collaborating researchers in the UIC School of Public Health, each of which was freeze-dried. To accomplish this, each sample was removed from the freezer and had the parafilm and original lid removed. A piece of aluminum foil was placed over the opening of each jar, and a similar lid to the original but with approximately a 4cm diameter hole removed from the center, was used to close each jar and secure each piece of foil. Then, a small capillary tube was used to poke at least 100 small-diameter holes in the aluminum foil. Each sample was then placed in a VirTis BenchTop 2K freeze dryer (SP Scientific, Gardiner, New York) until samples were

completely dry. Samples were then removed from the freeze drier, and placed into glass vials for analysis by several laboratories.

3.2. Sample Preparation for Gamma Spectroscopy

Each sample was ground to a uniform fine texture using a mortar and pestle. The samples were then transferred to polypropylene vials for use in the gamma detector. Each vial was labeled with the full sample name, and the mass of each dry, empty vial was recorded. The vial was then partly filled with sediment, and packed down by tapping the closed vial on a firm surface; this was repeated until sediment reached the level of the bottom of the vial cap. The vial was then capped, cleaned on the outside with methanol, and the mass of the full vial was obtained and recorded. The exterior of each vial was cleaned again with methanol before placing into the gamma detector.

3.3. Counting

Each sample was placed in one of two identical high-purity Ge well detectors (Model GWL-170-15-LB-AWT, EG&G Ortec, Ametek, Inc.). The twin detectors have 15mm diameter wells. All sections for each core were measured on the same detector. Lake Superior sites have up to 27 samples per site and each site took up to 5 weeks to measure on one detector. For every sample measured the gamma spectrometer recorded a data file containing the counts of gamma emissions detected in up to 4,000 energy channels. Each sample was counted for approximately 24 hours at least, with a bias toward longer counting times for deeper sections within a given core.

3.4. Calculation of Isotope Activities

Four isotopes are of primary interest for this project, with gamma emissions measured at the following photopeak energies: ^{210}Pb at 46.5keV, ^{226}Ra at 186.2keV, ^{241}Am at 59.7keV and ^{137}Cs at 661.6keV (Browne 2003, Basunia 2006, Browne and Tuli 2007, Singh et al. 2011). Activities for each nuclide of interest in each sample are calculated using the following steps:

The first step was to identify 5 to 10 energy channels which represent peaks in the gamma spectrum at the target energies.

Second, the average background was calculated by averaging the gamma counts in the 5 channels below the peak and the 5 channels above the peak.

Third, the net peak counts were calculated as a sum of the total counts in the peak minus the sum of the total average background counts beneath the peak.

The fourth step consisted of a statistical validity test for the peak. If the net peak count was greater than the detection limit, which is obtained by taking three times the square root of the number of background counts under the peak, the net peak count was considered statistically significant. Otherwise the activity is reported as less than or equal to the detection limit for that sample, in Bq/kg.

Fifth, counts per second for both the detection limit and the measured activity were calculated by dividing net peak counts or detection limit counts by the number of live-time seconds the sample was counted.

Sixth, decays per second were calculated by dividing counts per second by the empirically-determined detector efficiency at the energy of interest using the height of each sample.

Finally, specific activities in becquerels per kilogram (Bq/kg) were calculated by dividing the decays per second by the sample weight.

The activity calculation produces an activity (Bq/kg) as of the time of the gamma spectrometry measurement. In order to use the activities in a dating model, these activities must be adjusted to account for decay which has occurred from the time of collection to time of gamma spectrometry measurements. The calculation for this is given by

$$\text{Adjusted Activity } \left(\frac{\text{Bq}}{\text{kg}}\right) = \frac{\text{Measured Activity } \left(\frac{\text{Bq}}{\text{kg}}\right)}{e^{-\lambda t}} \qquad \text{Equation 1}$$

where λ is the decay constant for the respective radionuclide, calculated as

$$\lambda = \frac{\ln(2)}{\text{half life (years)}} \qquad \text{Equation 2}$$

and t is the time from sample collection to gamma spectrometry measurement in years.

3.5. CIC Dating Model

One model for deriving sedimentation rates and sample dates from a sediment core's profile of ^{210}Pb activity is known as the constant initial concentration (CIC) model. The primary assumption with this model is that all sediments throughout the core had a constant initial concentration; and therefore, the supply of ^{210}Pb varied directly with changes in sedimentation rate. Using the

method of Appleby (2001), dates are calculated for samples using the following formula:

$$C(z) = C(0)e^{-\lambda t} \quad \text{Equation 3}$$

which can be re-written to yield dates as follows:

$$t = \frac{1}{\lambda}\ln\left(\frac{C(0)}{C(z)}\right) \quad \text{Equation 4}$$

and sedimentation rate (r) is defined as:

$$r = \lambda M \quad \text{Equation 5}$$

where M is the slope of the best-fit line of dry mass vs. ln[C(0)/C(z)].

For this study, CIC dates and sedimentation rates are calculated for the entire profile, assuming a constant sedimentation rate, as well as by using 2- or 3-slope variations to determine if the sedimentation rate has changed throughout the profile.

3.6. CRS Dating Model

Another widely-used ^{210}Pb dating model is known as the constant rate of supply (CRS) model which was pioneered by Krishnaswami et al. (1971). This model assumes a constant rate of ^{210}Pb deposition throughout time, though the sedimentation rate may change. Under this model, such changes in sedimentation rate would result in changes in initial concentration of the nuclides of interest. The dating under this model is performed according to the following method from Appleby (2001):

$$A(m) = A(0)e^{-\lambda t} \quad \text{Equation 6}$$

where m is the depth of the sample, and A(0) and A(m) are calculated by:

$$A(0) = \int_0^\infty C(z)\mathrm{d}z \qquad \text{Equation 7}$$

where $A(0)$ is the cumulative amount of ^{210}Pb in the entire profile, and

$$A(z) = \int_z^\infty C(z)\mathrm{d}z \qquad \text{Equation 8}$$

where $A(z)$ is the cumulative amount of ^{210}Pb to sediment depth z.

Time in years since deposition is then found by

$$t = \frac{1}{\lambda} ln\left(\frac{A(0)}{A(z)}\right) \qquad \text{Equation 9}$$

Finally, sedimentation rate is found by

$$r = \lambda M \qquad \text{Equation 10}$$

where M is the slope of the best-fit line of cumulative dry mass vs. $ln[A(0)/A(z)]$.

Similarly to the CIC model, for each sample, CRS calculations are performed assuming a uniform slope for all points in addition to performing two- and three-slope calculations to ascertain changes in sedimentation rate.

3.7. Focus Factors

For each core, ^{210}Pb focus factors were calculated by dividing the total measured inventory of unsupported ^{210}Pb by 34.4 dpm/cm^2, which is the expected value of the "standing crop" of atmospheric ^{210}Pb deposition (Simcik et al. 1996). This yields a unitless positive ratio that describes sediment movement. Values less than unity, having less unsupported ^{210}Pb than expected, are areas where sediment either was not deposited or has moved away since deposition. In contrast, values

above unity are areas where sediment has moved into the area, thereby increasing the unsupported ^{210}Pb inventory above the expected value.

Another method for calculating focus factor utilizes ^{137}Cs to perform a similar calculation. Here, the measurements described in a technical memorandum by Robbins (1985) are utilized, along with a decay function to estimate the deposition since the memorandum was published to obtain an expected inventory of ^{137}Cs for Lake Superior, which in this case is 0.21 Bq/cm^2. The total measured inventory of the ^{137}Cs in each core is then divided by this value to obtain the ^{137}Cs focus factor. This quantity was not calculated for cores without visible ^{137}Cs peaks, as the ratio would be too biased toward zero, as part of the ^{137}Cs inventory is obviously missing.

3.8. Integration of Previous Study Data into GIS

Each of the previous studies that dated sediment cores in Lake Superior provided spatial coordinates in latitude and longitude. However, none of these studies except Johnson et al. (2012) provided the method for collection of the spatial data, and none provided the horizontal datum which the coordinates were reported in. Therefore, before integration into GIS for spatial analysis, a determination of the most likely horizontal datum was made in the following manner.

For the samples collected in the Great Lakes after World War II but prior to 1977, the primary method of spatial location was by plotting LORAN time delay (TD) signals on a navigational chart, and then extrapolating to the chart's graticule to obtain coordinates in latitude and longitude (Frank 1983). For Lake Superior, the American versions of these charts, published by NOAA, were based on either

the US Standard Datum of 1902, or the North American Datum of 1927 (NAD 27). Utilizing the reported latitude and longitude of the sample points in question, and a table constructed from map title block information from historical NOAA charts, the horizontal datum of the largest-scale chart for that approximate location were obtained. Coordinates were then imported to ArcGIS as either US Standard Datum or NAD 27 points. The NAD 27 coordinates were converted to WGS 1984 coordinates using the Project tool in ArcGIS. For US Standard Datum coordinates, a custom conversion grid was provided by the US National Geodetic Survey for use in publicly-available NADCON conversion software (Cindy Craig, Personal Communication) to convert the coordinates into the NAD 83 datum.

For samples collected after 1977, but before 1994, latitude and longitude coordinates were most likely obtained by automatic conversion by the LORAN receiver on-board the ship (Frank 1983). These conversions were accomplished by mathematical conversion from a LORAN spherical coordinate system to a geocentric Cartesian coordinate system, and then to the desired ellipsoidal geographic coordinate system such as WGS 1972 or WGS 1984 (RTCM 1981, Williams and Last 2003). For the purposes of this study, all points collected from 1977 to 1985 were assumed to be reported in WGS 1972, and all points from 1986 to 1994 were assumed to be reported in WGS 1984.

For samples collected in 1994 and later, all coordinates were assumed to be reported in WGS 1984 geographic coordinate system. This is the coordinate system utilized by GPS systems which became commercially available in 1994, and all

NOAA navigational charts had been updated to the WGS 1984 datum by that point. Furthermore, by 1996, any ships still using LORAN receivers to provide coordinates would also be in WGS 1984, as these receivers were programmed by then to use WGS 1984 to enable direct use with GPS-derived locations (Fisher 1996).

4. Results

4.1. Activity Profiles

The results of the gamma spectrometry measurements are presented in Figure 5 through Figure 13. For all profiles, the activities of the four measured isotopes are shown by the average depth of the section. The expected trends for the isotopes are as follows: ^{210}Pb should have highest activities near the surface, declining in an exponential manner until secular equilibrium with its parent isotope is reached, and then a constant value for the rest of the sections down the core. ^{226}Ra activities are generally approximately constant throughout the core. ^{137}Cs and ^{241}Am activities both are expected to peak below the surface at the same depth.

Core 2011-S001MC, which is the nearest sample in this study to Whitefish Bay and the St. Mary's River outlet from Lake Superior, was anomalous with regard to the activity profile compared to the other samples (Figure 5). First, this core had no ^{241}Am detected, and there was no apparent peak of ^{137}Cs. While the general shape of the ^{210}Pb and ^{226}Ra profiles are as expected, the relatively low activity values for ^{210}Pb in the top sections, along with the shallow depth at which equilibrium is reached, suggest that this core is not located in a depositional area, and accordingly, recent sediments have not been preserved. Because of the lack of detectable ^{241}Am, and the lack of sufficient ^{210}Pb data, dating models were not applied to the data from this core.

Core 2011-S002MC, located east of Caribou Island in the Whitefish sub-basin, generally fit the expected shape for each isotope profile (Figure 6). The

unsupported ^{210}Pb, as determined by the Ra-subtraction method, was detectable until the sixth section at an average depth of 2.75cm. The ^{137}Cs and ^{241}Am peaks are not visible in this core, which suggests the loss of some quantity of surface sediments. Because this core is situated well within a recognized depositional area, the simplest explanation for this loss of sediment is disturbance of the flocculent layer during sampling. By utilizing the sedimentation rate from the CRS model (discussed later) and the onset of ^{241}Am, and assuming the density of the missing sediment is the same as the density in the top section, approximately 1.9 cm, which corresponds to 0.205 g/cm^2, of sediment were lost at core S002.

Core 2011-S008MC, which is located in deep waters east of the Keweenaw Peninsula, also has a radioisotope profile (Figure 7) that conforms to expected shapes, but appears to be missing surface sediment. The unsupported ^{210}Pb exists to the eighth section at a depth of 3.75cm. The peaks for ^{137}Cs and ^{241}Am both are not visible in this profile, which is the primary indicator that some amount of sediment is missing from this core. However, utilization of the ^{137}Cs and ^{241}Am onsets in conjunction with the density data and the CRS and CIC model-derived sedimentation rates did not yield a valid estimate of the quantity of missing sediment. This implies that the CRS and CIC models may not be appropriate for this location, and sedimentation rates provided here should be used with caution.

Core 2011-S011MC is located northeast of Isle Royale in the Isle Royale sub-basin. The shapes of all four isotope profiles (Figure 8) match the expected trends. Unsupported ^{210}Pb is found in the top 14 sections, to a depth of 8.5cm. The peaks of

^{137}Cs and ^{241}Am are clearly visible, and occur in the same section at 2.25cm depth. Assuming that any lost sediment has the same density properties as the top section, and utilizing the sedimentation rate determined from the CRS model, a loss of 0.14cm (0.023 g/cm^2) would be required to obtain a date of 1954 at the ^{241}Am onset.

Core 2011-S012MC is located between Isle Royale and the Keweenaw Peninsula in the Isle Royale sub-basin. The activity profile (Figure 9) for this core has all of the expected shapes with clear patterns. Unsupported ^{210}Pb exists in the top twelve sections, to a depth of 6.5 cm. The ^{137}Cs and ^{241}Am peaks are well defined and well aligned. This is one of the two cores where a deep sample at 42 cm depth was obtained; here it shows constant activity of ^{210}Pb and ^{226}Ra as expected. Assuming a linear decrease in sediment density towards the surface, a value for the average density of potential lost sediment can be obtained. Using this method and the sedimentation rate obtained from the CRS model, 1.3 cm (0.161 g/cm^2) of sediment would need to be missing in order to align the ^{137}Cs peak with 1963.

Core 2011-S016MC is located in the western part of the lake in the Chefswet sub-basin, southwest of Isle Royale. The activity profile (Figure 10) shows the expected general trends with depth. The unsupported ^{210}Pb is present for nine sections to a depth of 4.25 cm. The peaks for ^{137}Cs and ^{241}Am are not distinct in this core. For purposes of dating and validating ^{210}Pb results, the ^{137}Cs peak at 1.75 cm depth, with a corresponding local maximum in ^{241}Am, is used. With this assumption in mind, and assuming a linear trend in surface sediment density, the amount of sediment loss required to place 1963 at this ^{241}Am and ^{137}Cs maximum is

0.85 cm (0.093 g/cm^2). Another explanation for the obscurity in the ^{137}Cs and ^{241}Am data is the homogenization of the two casts. Evidence of local-scale variation in this part of the lake has been documented by Johnson et al. (2012), and homogenization of such varied sediment would explain the apparent "double-peak" seen here.

Core 2011-S019MC, located in the Duluth sub-basin north of the Apostle Islands, has all expected features on the activity profile (Figure 11). The first eleven sections contain unsupported ^{210}Pb, to a depth of 5.5 cm. The ^{137}Cs peak is clearly visible and has the expected shape. The ^{241}Am peak is less apparent, but the ^{241}Am activity in the sections above, below, and including the ^{137}Cs peak are all within error of one another, suggesting the existence of a well-aligned if poorly-defined ^{241}Am peak. The ^{137}Cs peak allows an estimate of lost sediment. Assuming any lost sediment had the same density as the top section, and using the sedimentation rate from the CRS model, 1.1 cm of sediment must have been lost to align the ^{137}Cs peak with 1963.

Core 2011-S022MC is located in far western Lake Superior, in the Duluth sub-basin near the cities of Duluth, Minnesota and Superior, Wisconsin. This profile (Figure 12) also exhibits all of the expected features previously discussed. This core has the deepest unsupported ^{210}Pb in this study, with unsupported ^{210}Pb in the top 17 sections, to a depth of 11.5 cm. The peak in ^{137}Cs is readily apparent, and the maximum activity of ^{241}Am occurs in the same section as the ^{137}Cs peak. Assuming any lost sediment had the same density as the top section of the core and using the sedimentation rate from the CRS model, the estimated lost sediment

required to align the peak with 1963 is 2.89 cm. This relatively large disturbance of surface sediment may explain the subsurface peak in ^{210}Pb visible in the profile. Alternatively, this apparent subsurface peak may be due to the effects of near-surface sediment disturbance during sampling, or multiple-cast homogenization as discussed previously.

Finally, core 2011-S114MC is located at the deepest point in Lake Superior, in the southern part of the Caribou sub-basin. The profile for this core (Figure 13) displays patterns consistent with a very low sedimentation rate, as expected for such deep bathymetry. One example is that unsupported ^{210}Pb is found only in the top 2 cm of the core. This core also included a deep section at 42cm, and the ^{210}Pb and ^{226}Ra activities are similar at that depth to the activities of those isotopes in sections 5-25 (2-25 cm), which is the expected result. Notably, the ^{210}Pb and ^{226}Ra values fluctuate with depth more than any other core in this study. The ^{137}Cs peak is not visible in this core, and the highest 137Cs activity occurs at the sediment-water interface. While a peak of ^{241}Am is visible, all three activity values for ^{241}Am are within error of each other, and therefore the validity of this "peak" is suspect. The ^{241}Am onset was utilized to attempt an estimate of lost sediment. However, using the sedimentation rate from the CRS model, no valid amount of lost sediment could be obtained regardless of assumptions regarding density of lost sediment.

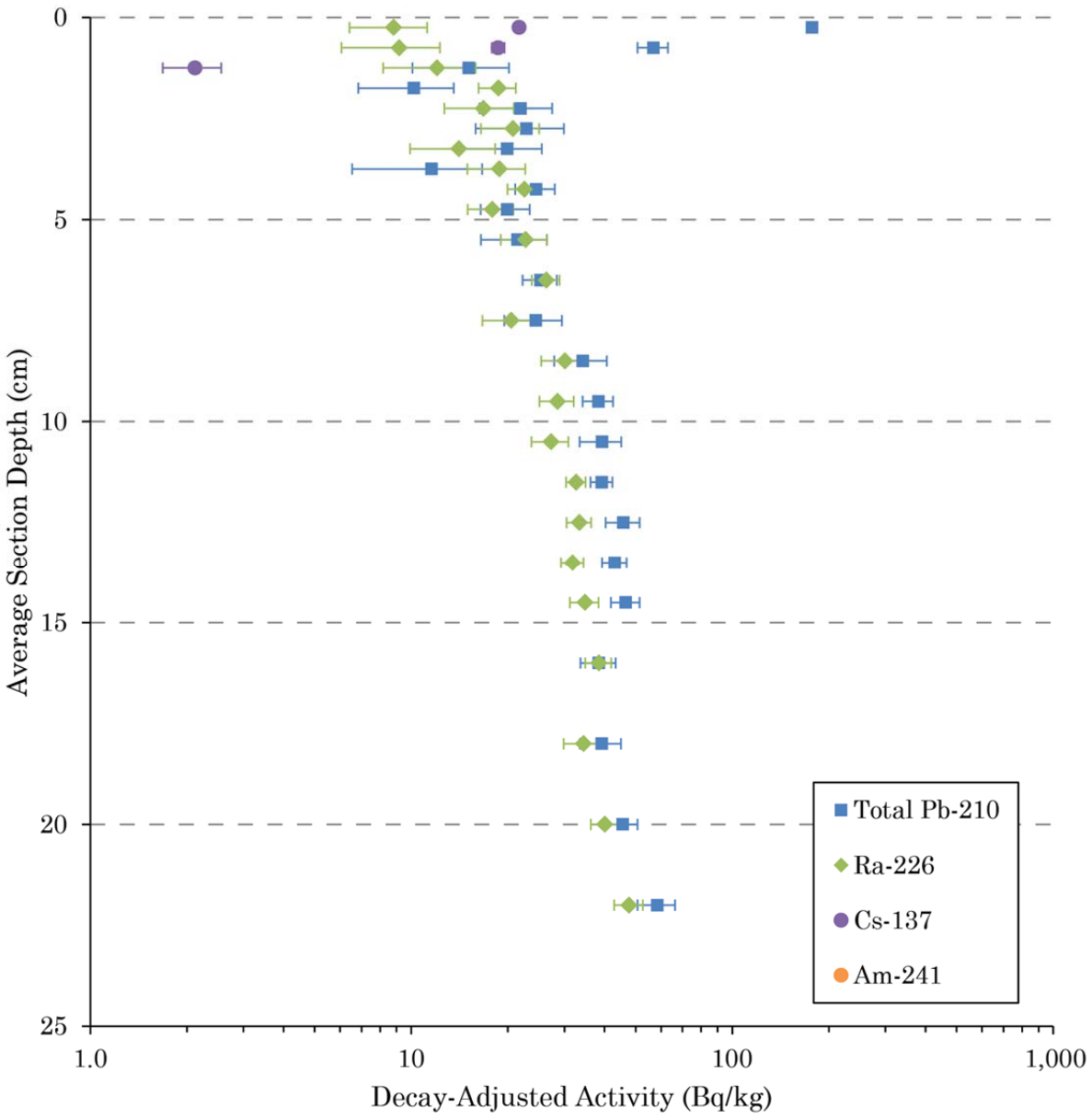

Figure 5. Activity Profile for core 2011-S001MC

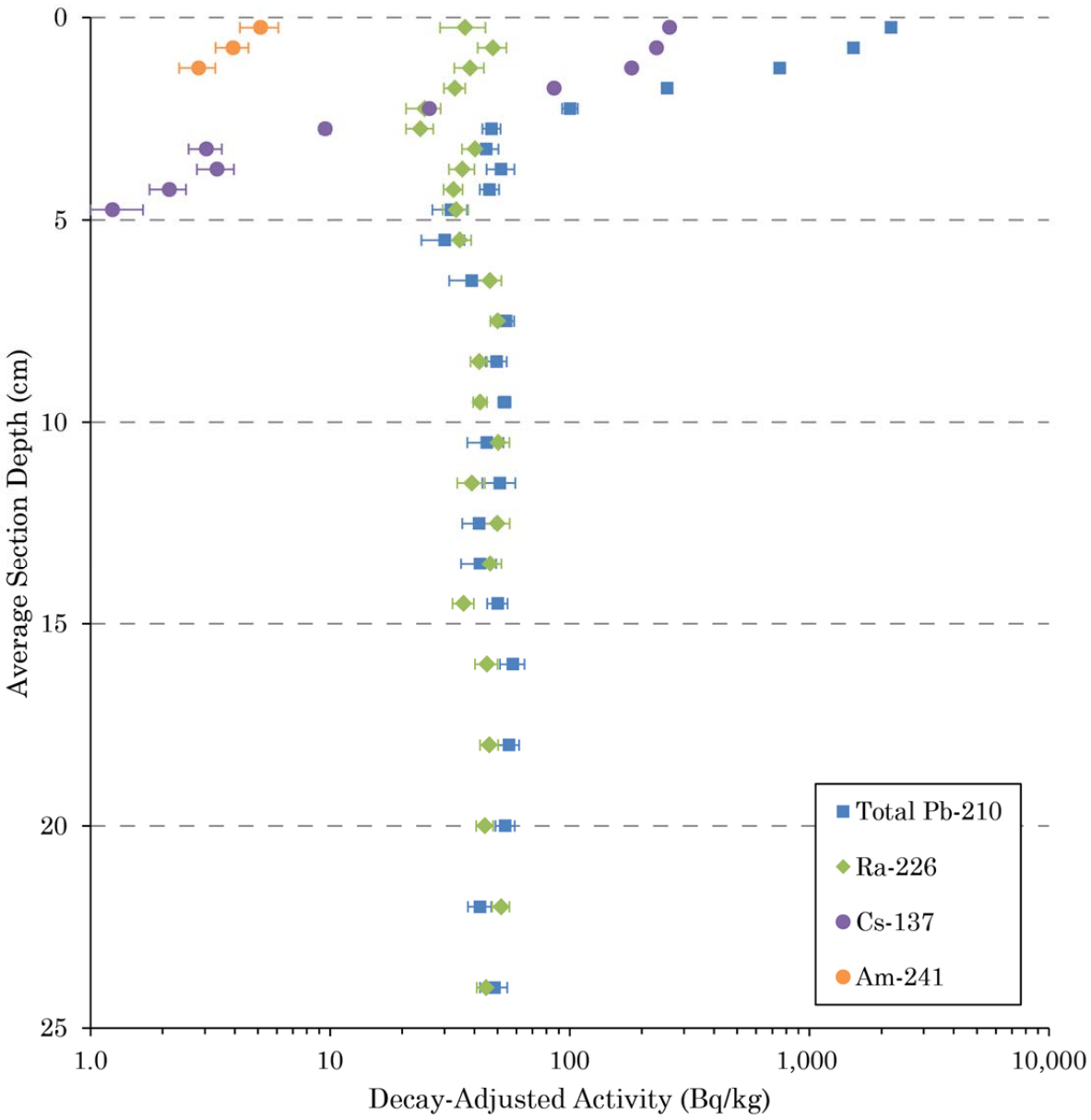

Figure 6. Activity Profile for core 2011-S002MC

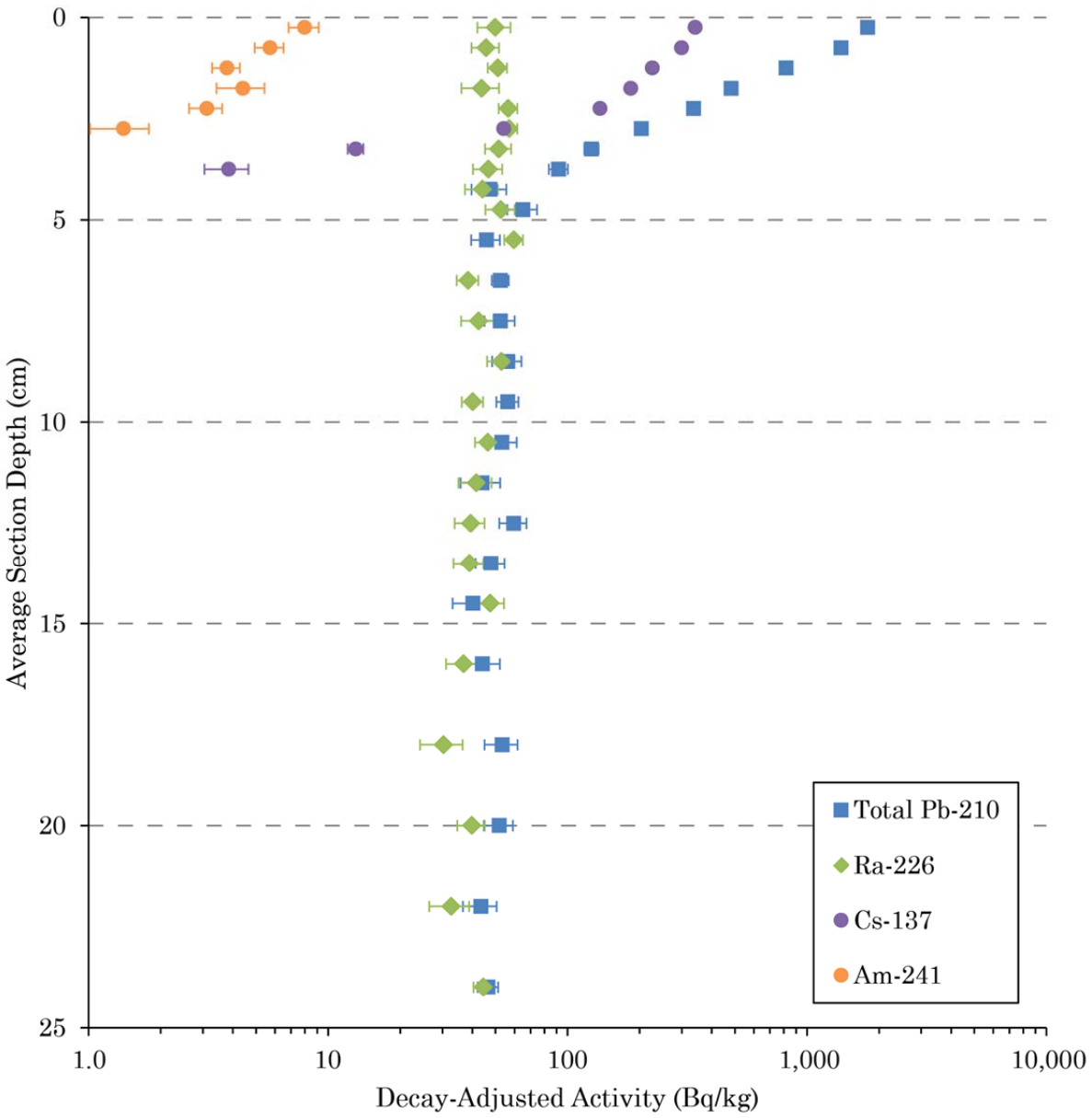

Figure 7. Activity Profile for core 2011-S008MC

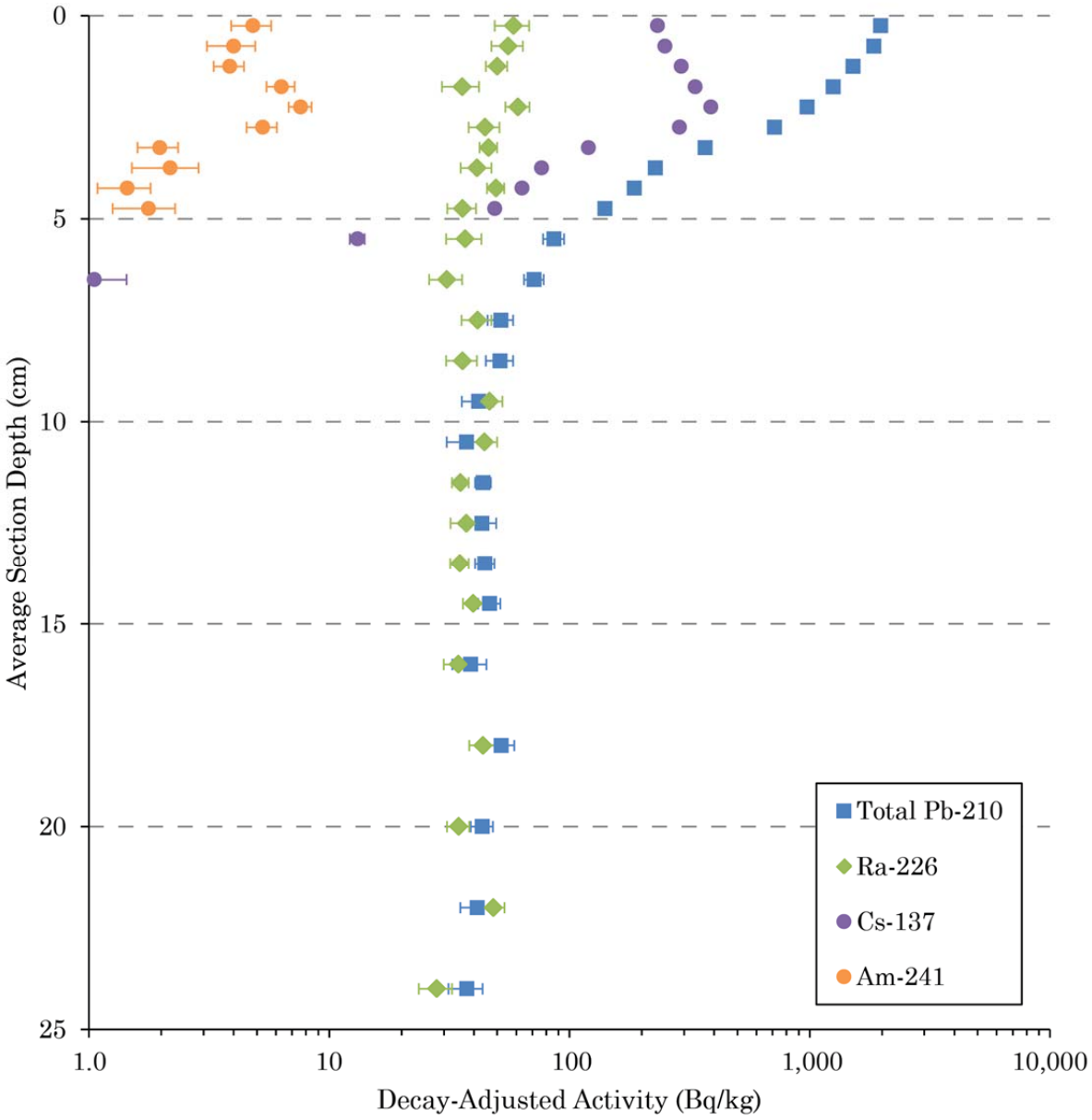

Figure 8. Activity Profile for core 2011-S011MC

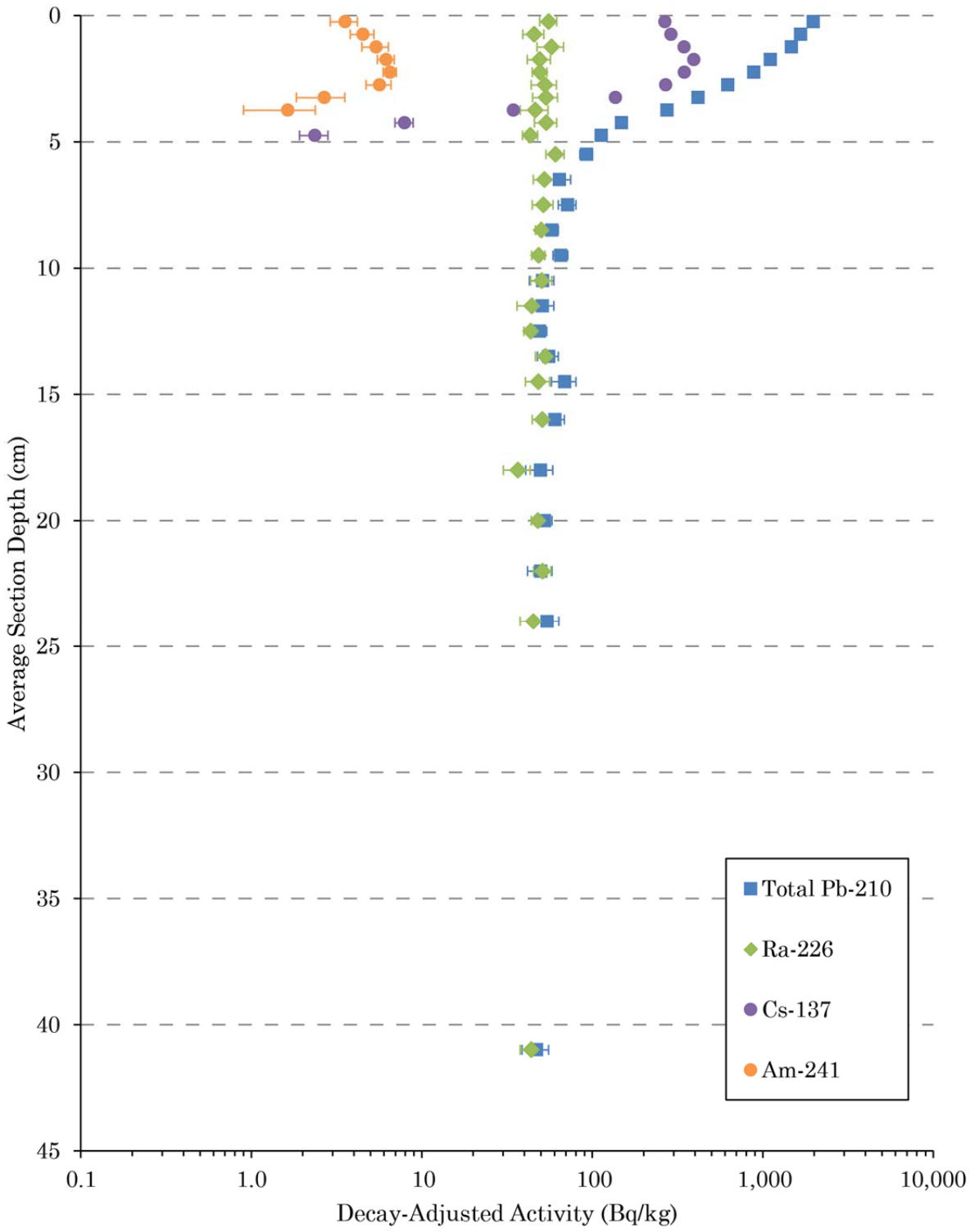

Figure 9. Activity Profile for core 2011-S012MC

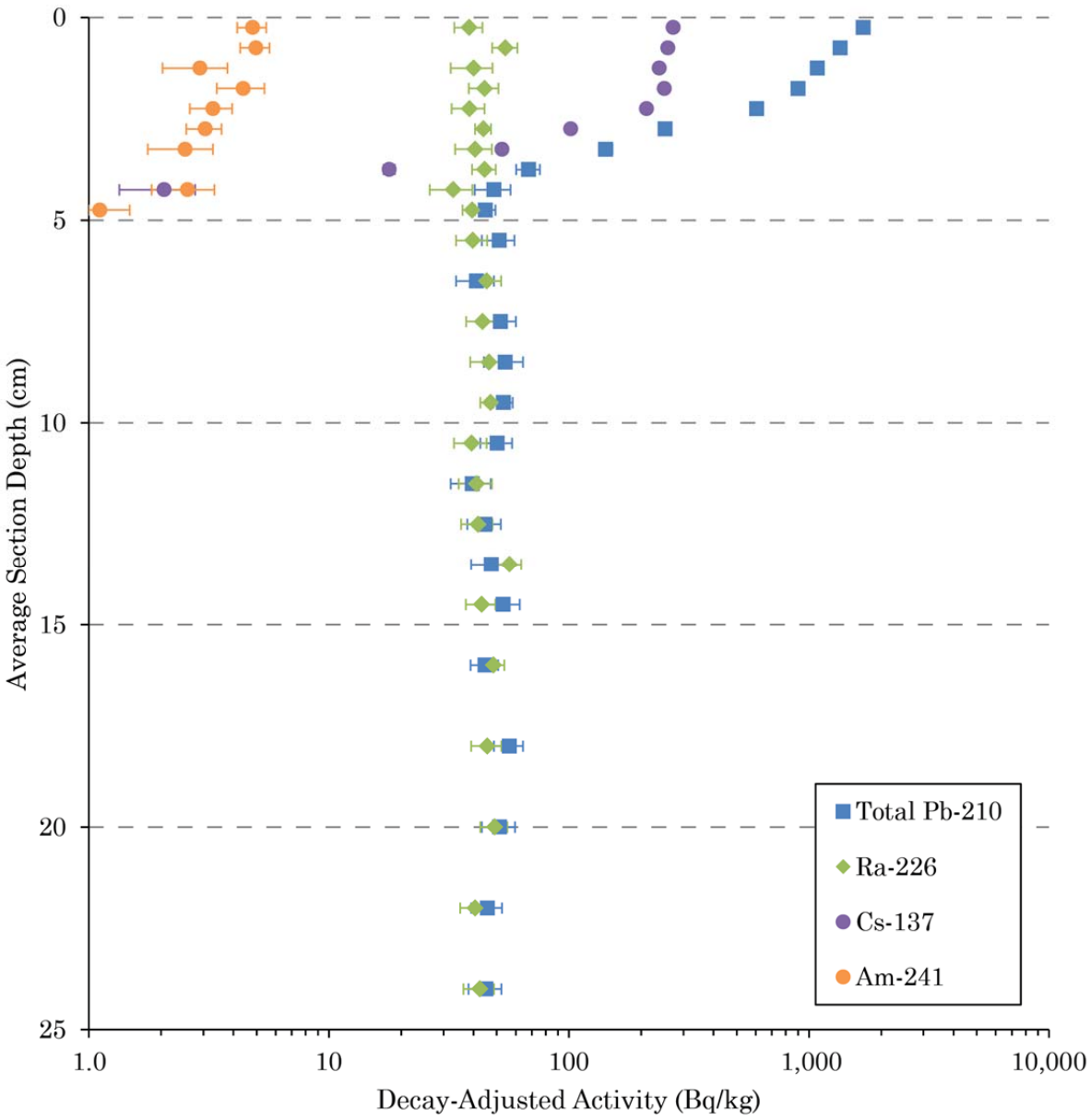

Figure 10. Activity Profile for core 2011-S016MC

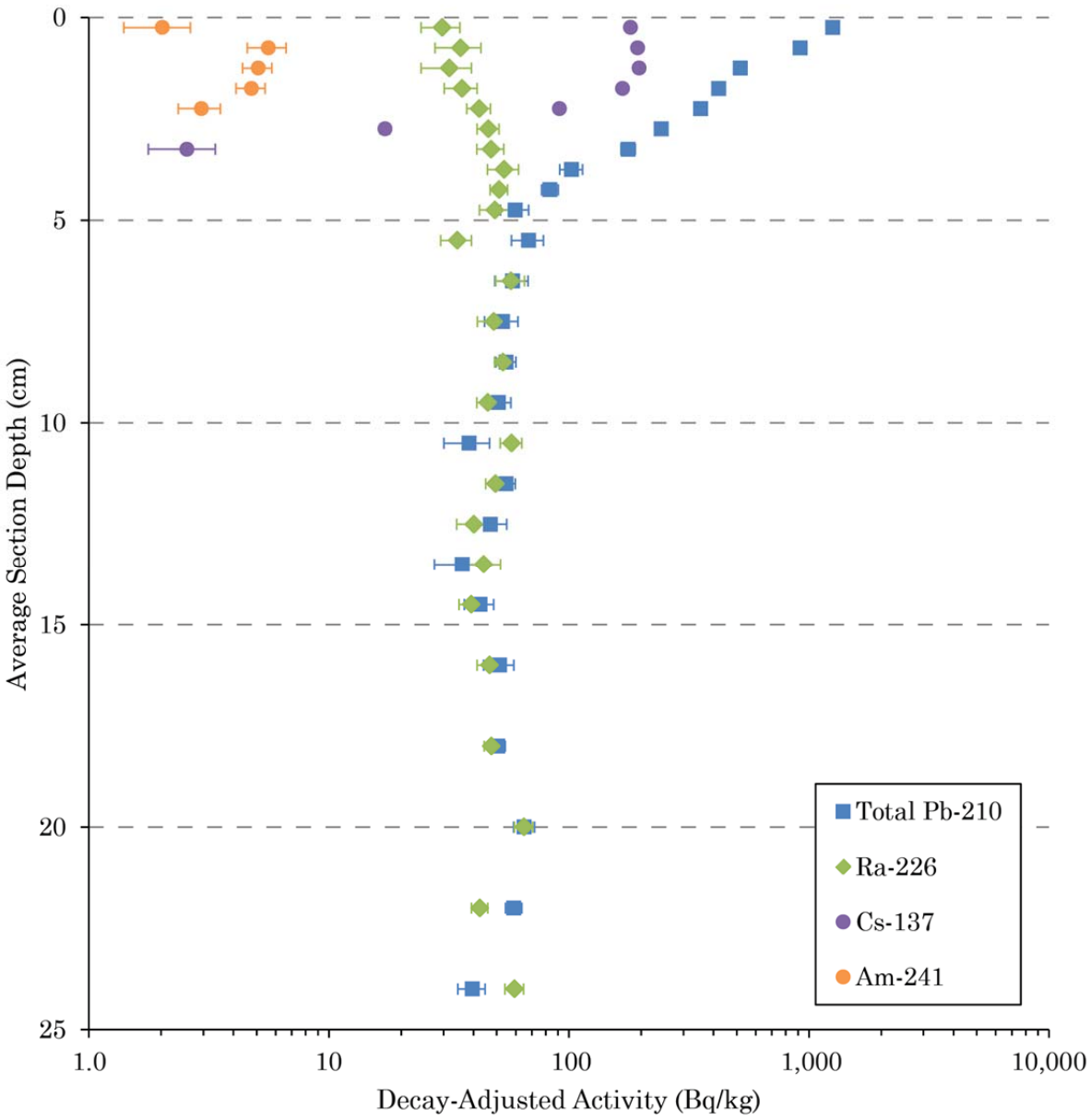

Figure 11. Activity Profile for core 2011-S019MC

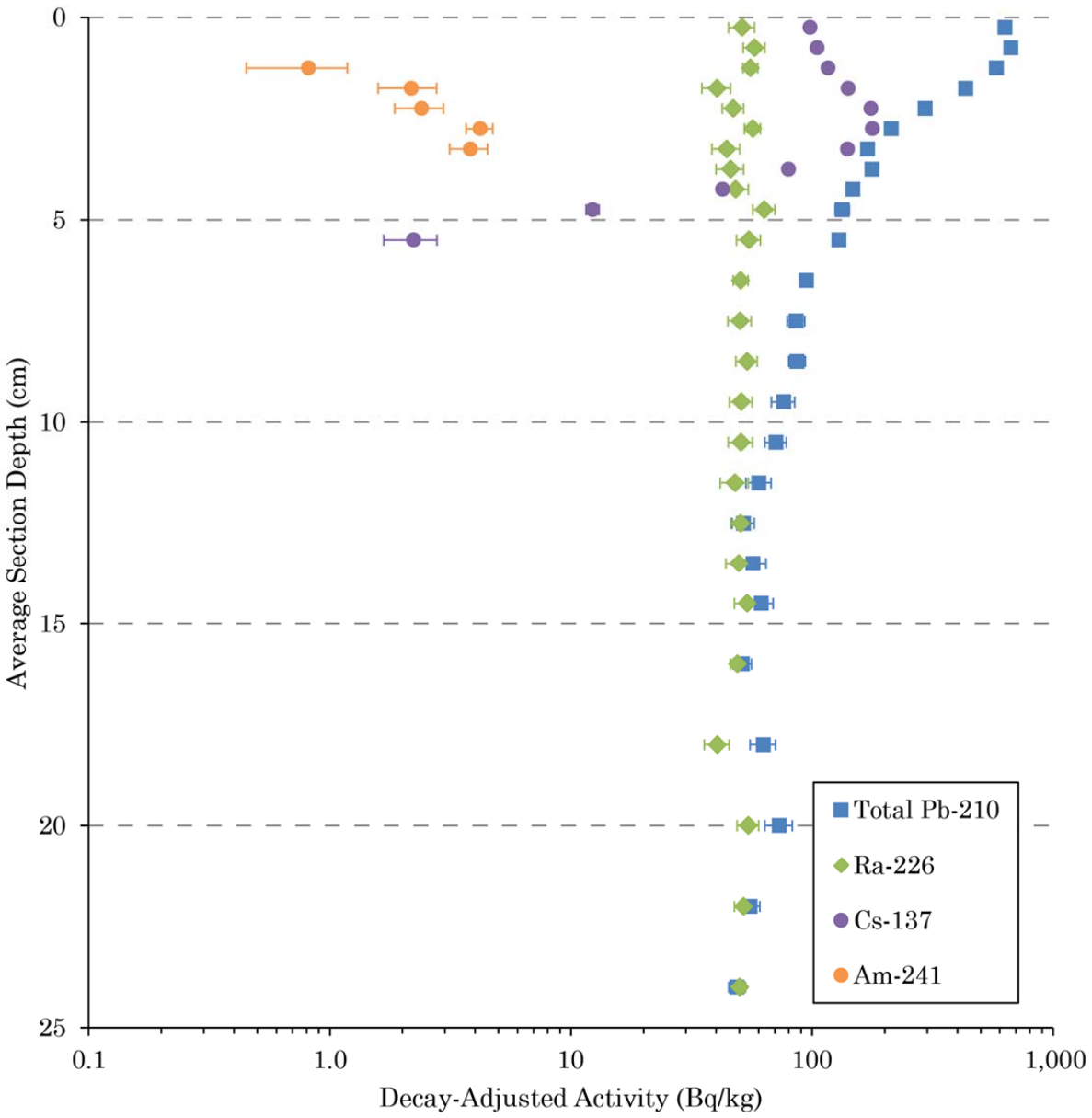

Figure 12. Activity Profile for core 2011-S022MC

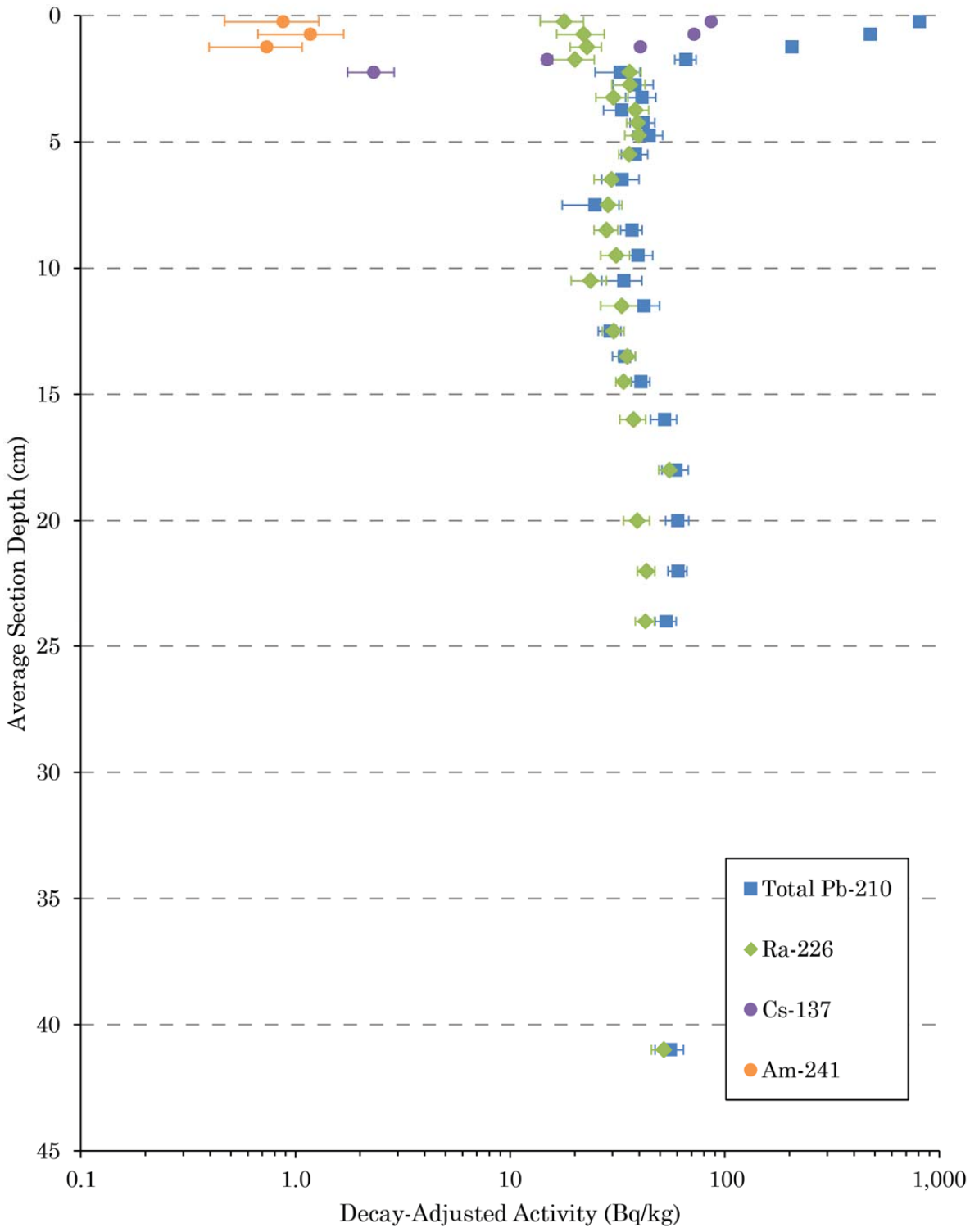

Figure 13. Activity Profile for core 2011-S114MC

4.2. Dating Model Results

Determination of sedimentation rates, and subsequently calendar dates where possible, was undertaken for eight of nine cores. For each core, CRS and CIC one-slope models were evaluated first, to determine if evaluation of a two- or three-slope version was warranted. In all cases, the single-slope version of both models resulted in an R^2 value of 0.88 or higher, and all cores except S114 had at least one of the single-slope models with $R^2 = 0.97$ or higher. Therefore, multiple-slope models were deemed unnecessary for this study.

For all models, the amount of unsupported ^{210}Pb was determined by the Ra-subtraction method.

At core 2011-S002MC, the results (Figure 14) of the CRS and CIC models were lines of cumulative dry mass vs. *ln*(A0/Az) or *ln*(C0/Cz) that were well-fit, with R^2 values above 0.99 in both cases. The sedimentation rates derived from these models (CRS: 0.0080 ± 0.0002 g/cm^2/y, CIC: 0.0076 ± 0.0002 g/cm^2/y) both have low standard errors. The CRS model has a slightly better fit for these data, and therefore the CRS-derived sedimentation rate is chosen as the primary result for determination of absolute dates, estimates of possible missing sediment, and for interpolation of sedimentation rates throughout the lake.

Core 2011-S008MC had more data points than S002, but had a similar fit of the lines of cumulative dry mass vs. *ln*(A0/Az) or *ln*(C0/Cz), with R^2 values over 0.99 for both models (Figure 15). The standard error for the sedimentation rates (CRS: 0.0069 ± 0.0001 g/cm^2/y, CIC: 0.0076 ± 0.0002 g/cm^2/y) is low for both models, but

lower for the CRS-derived rate. Accordingly, the CRS model will be used for dating and interpolation purposes.

Core 2011-S011MC had a greater difference between the two models, both in terms of the fits of the lines of cumulative dry mass vs. *ln*(A0/Az) or *ln*(C0/Cz) and in terms of the derived sedimentation rates. The CRS model had a better R^2 value at 0.97 compared to an R^2 value for the CIC model of 0.93 (Figure 16). This corresponds to a lower error in the sedimentation rates (CRS: 0.0228 ± 0.0012 g/cm^2/y, CIC: 0.0187 ± 0.0015 g/cm^2/y) for the CRS sedimentation rate. The sedimentation rates in core S011 are the highest of any core in this study by a factor of two. Because of the better fit in the CRS model, the CRS-derived sedimentation rate will be utilized in other calculations in this study.

Core 2011-S012MC is another core that is characterized by strong agreement between the two models in all aspects. The lines of cumulative dry mass vs. *ln*(A0/Az) or *ln*(C0/Cz) are well fit with R^2 values at or above 0.99 for both models (Figure 17). Accordingly, the sedimentation rates have low error values and are in almost exact agreement (CRS: 0.0096 ± 0.0002 g/cm^2/y, CIC: 0.0096 ± 0.0003 g/cm^{2}y). Due to the lower error value for the CRS result, the CRS-derived sedimentation rate will be used for the other calculations in this study.

Core 2011-S016MC is a core where the fit of the lines of cumulative dry mass vs. *ln*(A0/Az) or *ln*(C0/Cz) was also high for both models. The fit of the CRS model was slightly better (CRS: $R^2 = 0.99$, CIC: $R^2 = 0.98$) than for CIS, as seen in Figure 18. The error values in the sedimentation rates derived from these models are

correspondingly low (CRS: 0.0085 ± 0.0002 g/cm^2/y, CIC: 0.0085 ± 0.0004 g/cm^2/y). Despite almost exactly matching sedimentation rates for this core from the two models, the lower error values for the CRS-derived rate indicate that CRS is the appropriate model for this core.

Core 2011-S019MC has a distinct anomalous value at the deepest section of those determined to contain unsupported ^{210}Pb. This section has a high ^{210}Pb specific activity as determined by the Ra-subtraction method. Because of the inherent assumptions of the models, this influences the results of the CIC model to a greater degree than the CRS model, as seen in Figure 19. The CRS model, therefore, has a better fit than the CIC model (CRS: $R^2 = 0.97$, CIC: $R^2 = 0.89$). The error associated with the sedimentation rate form the CRS model is also lower (CRS: 0.0111 ± 0.0007 g/cm^2/y, CIC: 0.0094 ± 0.0011 g/cm^2/y). The CRS model is therefore the most appropriate for use in other calculations, due primarily to its better ability to handle the anomalously high activity value.

Core 2011-S022MC has the most sections containing unsupported ^{210}Pb of any core in this study, resulting in the highest number of data points for the CRS and CIC models. Both models provided a good fit for the line of cumulative dry mass vs. ln(A0/Az) or *ln*(C0/Cz), but the fit for the CRS model was slightly better (CRS: $R^2 = 0.97$, CIC: $R^2 = 0.95$), as shown in Figure 20. The sedimentation rate errors correspond to this difference in fit, such that the error on the CRS rate is smaller than for the CIC rate (CRS: 0.0330 ± 0.0014 g/cm^2/y, CIC: 0.0352 ± 0.0022

g/cm^2/y). Given the better model fit for the CRS results, the CRS-derived sedimentation rate was chosen for use in other calculations in this study.

Finally, core 2011-S114MC had the fewest sections containing unsupported ^{210}Pb in this study, with the exception of S001, which was likely not located in a depositional area. The regression lines for the two models fit the data similarly as both models had $R^2 = 0.94$ as shown in Figure 21. However, the error for the CRS-derived sedimentation rate was slightly lower than the error for the CIC results (CRS: 0.0074 ± 0.0014 g/cm^2/y, CIC: 0.0091 ± 0.0016 g/cm^2/y). Therefore, the CRS model results are selected for use in other calculations in this study.

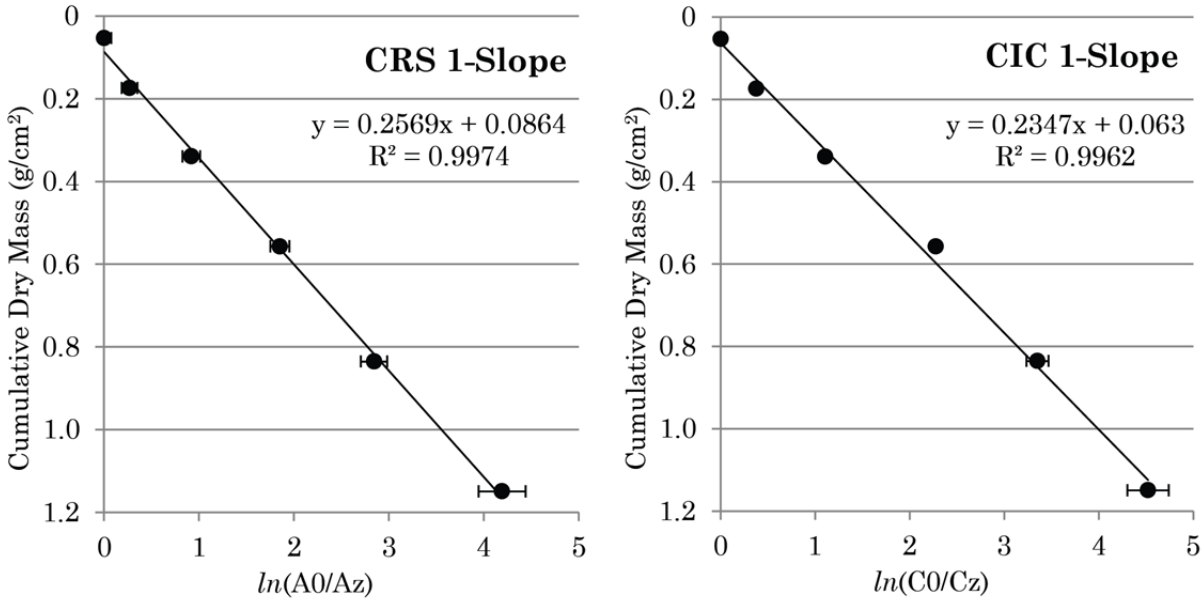

Figure 14. Model Results for core 2011-S002MC

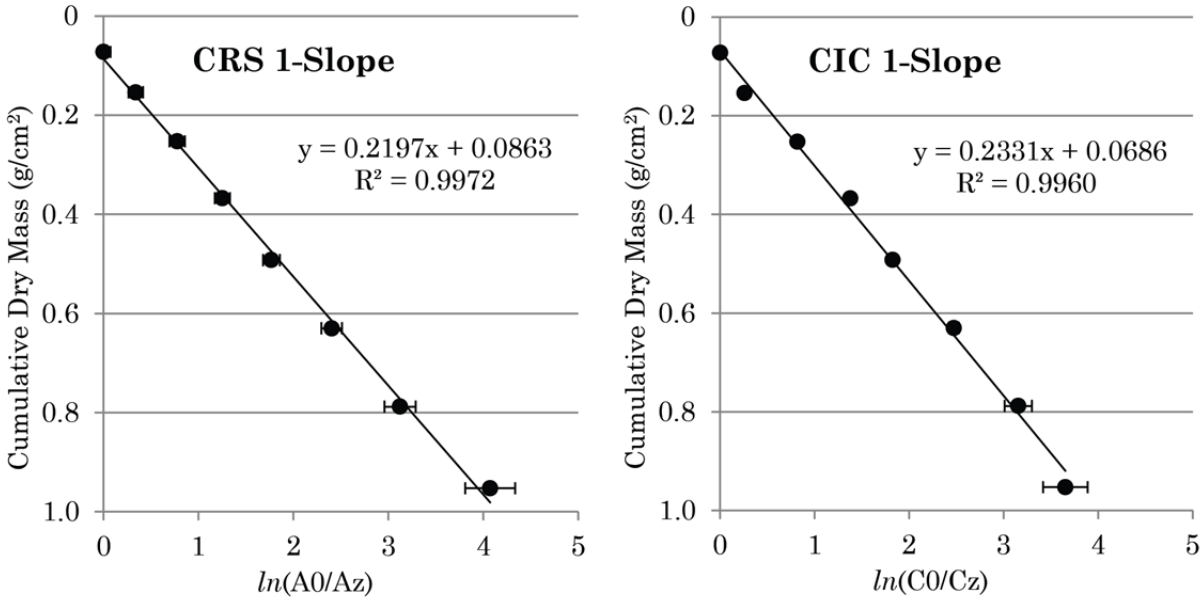

Figure 15. Model Results for core 2011-S008MC

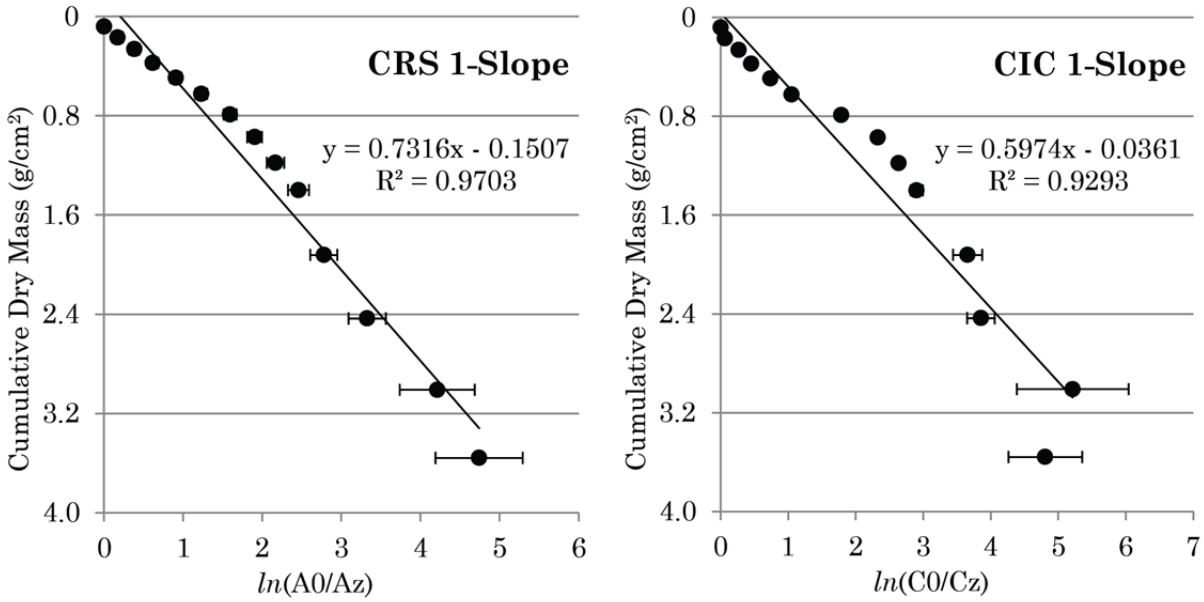

Figure 16. Model Results for core 2011-S011MC

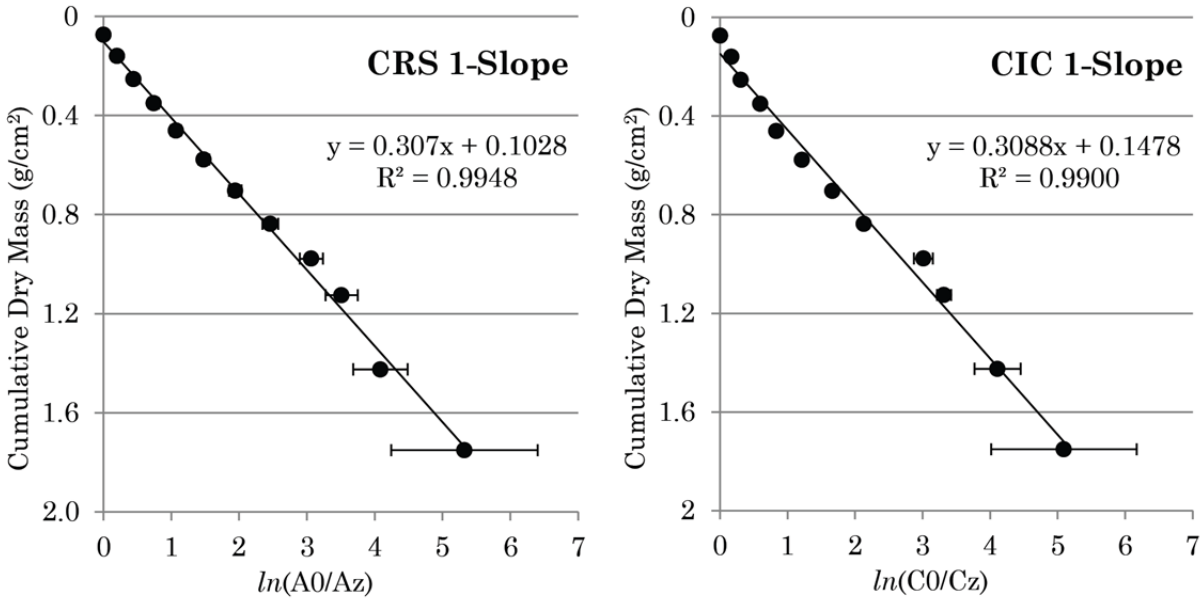

Figure 17. Model Results for core 2011-S012MC

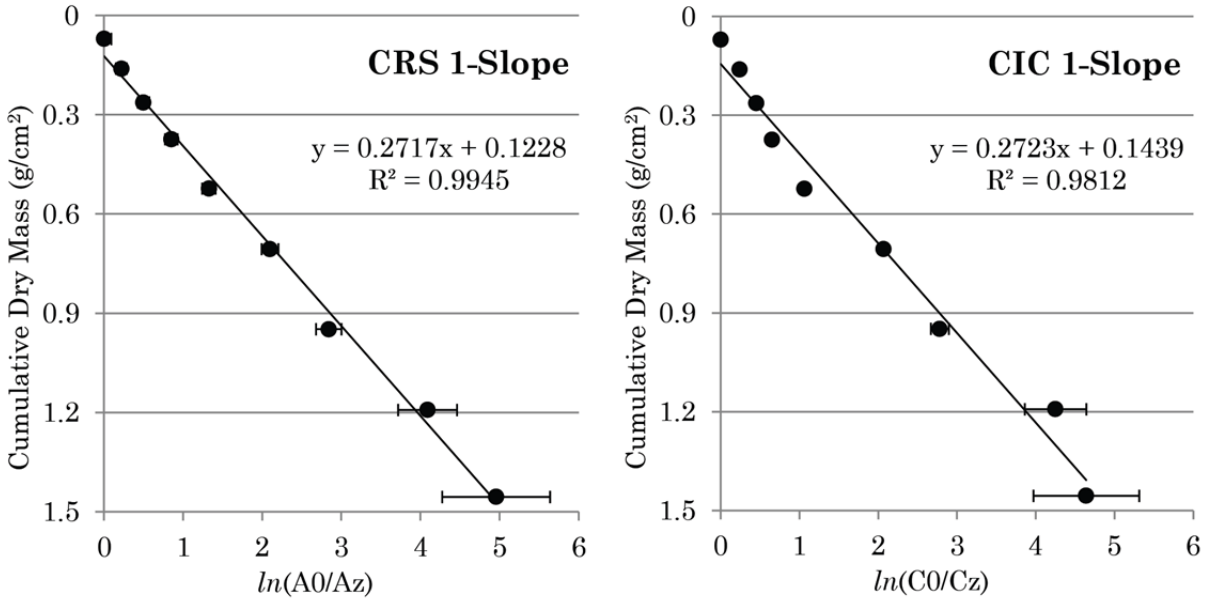

Figure 18. Model Results for core 2011-S016MC

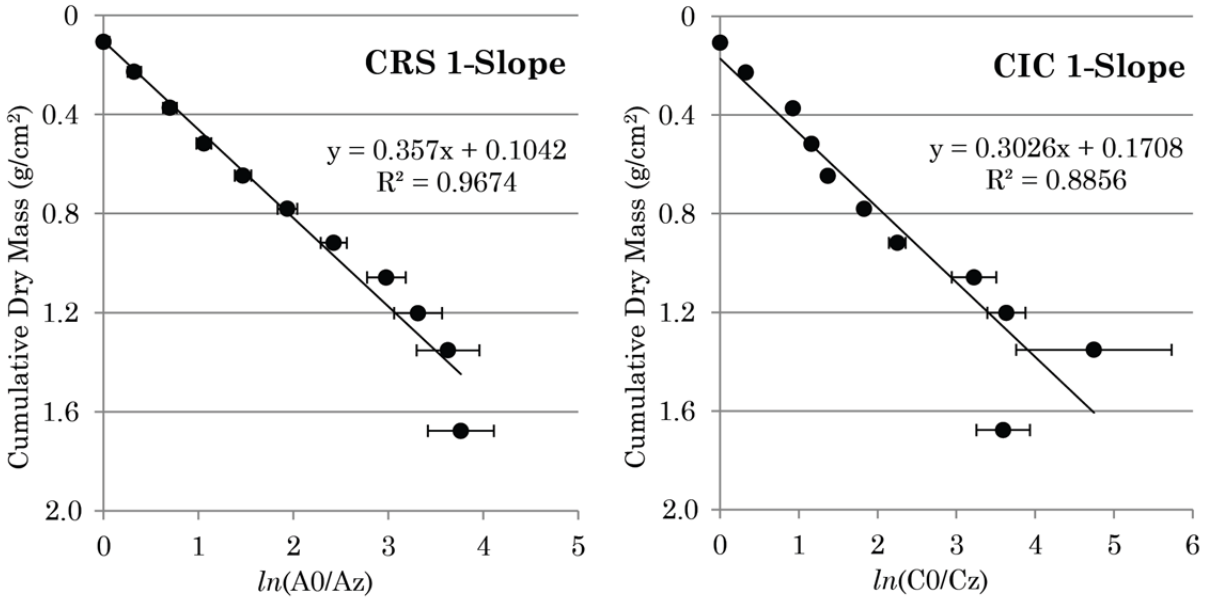

Figure 19. Model Results for core 2011-S019MC

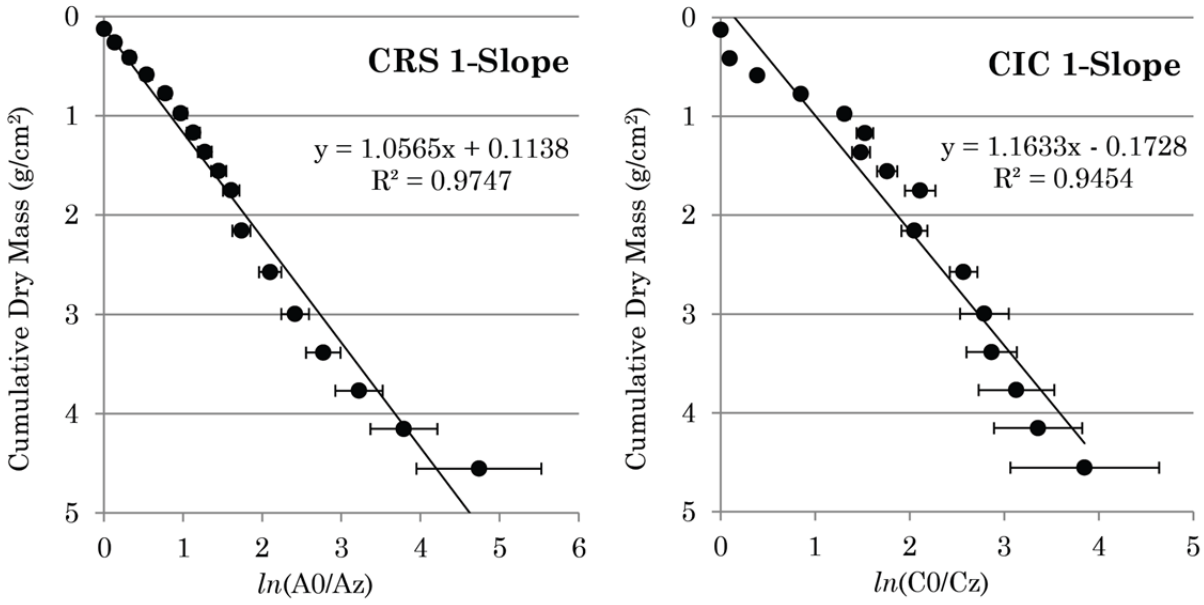

Figure 20. Model Results for core 2011-S022MC

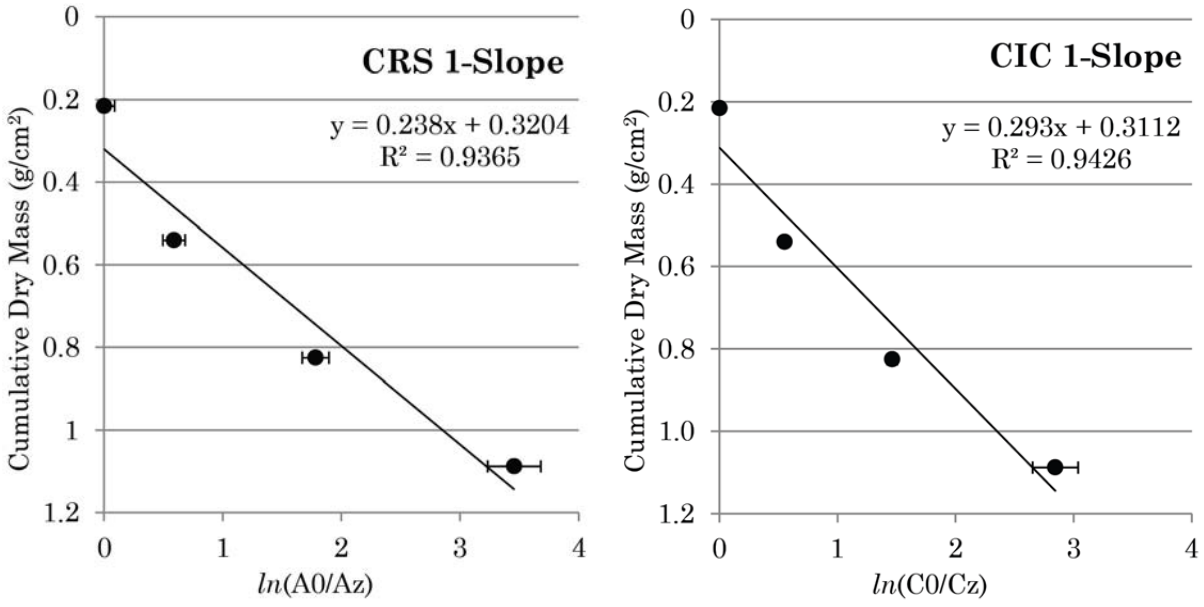

Figure 21. Model Results for core 2011-S114MC

4.3. Focus Factors

For all cores except 2011-S001MC, a ^{210}Pb focus factor was calculated. All focus factor results are reported in Appendix A, Table III through Table XI. The ^{210}Pb focus factors are expected to be near or below unity in many cores from this study if the hypothesis of missing surficial sediment is correct. With the exception of cores S011 and S012, having values of 1.72 and 1.38, respectively, all other cores do have values near or below unity.

In cores with a visible ^{137}Cs peak, a separate ^{137}Cs focus factor was calculated for the sake of comparison. Because all sites in this study besides S001 are situated in depositional areas, the ^{137}Cs focus factor is expected to be above unity. However, the same bias exists due to missing sediment, causing this method to also yield artificially low results. The cores with unexpectedly low ^{137}Cs focus factors are sites S016 and S019, with values of 0.77 and 0.52, respectively.

4.4. Sedimentation Rate Mapping

The locations for each of the cores reported in the literature were converted to a common coordinate system and brought into ArcGIS for analysis. One sedimentation rate was associated with each point. Where more than one sedimentation rate was reported at the same location with the same sampling date, rates for mapping were selected as follows: First, a rate determined using the CRS model was chosen for consistency when available. Second, if the authors interpreted a change in sedimentation rate, the contemporary rate was used. Finally, if more than two rates were reported, the median rate was selected. Once

all points had an associated sedimentation rate, the “Spline with Barriers” tool from the ArcGIS Spatial Analyst toolbar was utilized to fit a surface to the data points, utilizing the shoreline as a natural barrier such that points on one side of a topographic feature such as Isle Royale or the Keweenaw Peninsula did not affect the mapped rates on the other side of the feature. The output is shown in Figure 22 along with sampling locations for all samples for reference. Contours on this map are labeled in $mg/cm^2/y$ for map clarity.

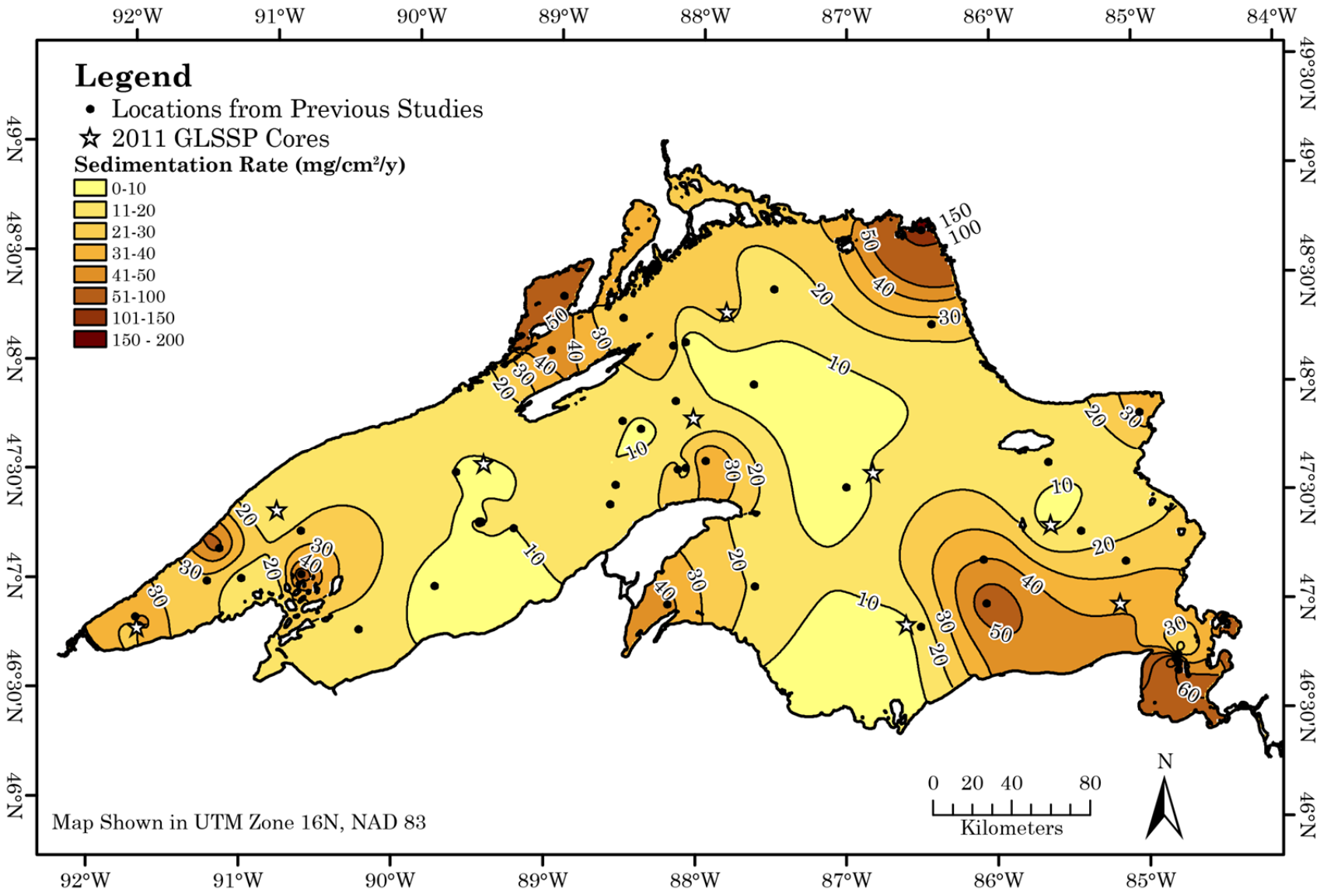

Figure 22. Sedimentation Rate Map for Lake Superior

5. Discussion

5.1. Comparison to Previous Sedimentation Rates

Core 2011-S001MC appears to be a non-depositional area, which is consistent with the delineation of depositional areas in Thomas and Dell (1978). This core is near the Whitefish sub-basin, but as no sedimentation rate was calculated, serves only to validate the classification of this area as non-depositional.

For core 2011-S002MC, the nearest comparable sample is core C-79 29BX from Evans et al. (1981) which has a sedimentation rate value of 0.014 g/cm^2/y, which is almost twice the value obtained in this study. However, such a discrepancy is reasonable given the highly variable bathymetry in the Whitefish sub-basin. Given the spatial uncertainties associated with the coordinates from the 1979 sampling efforts, in addition to the spatial uncertainties inherent in lowering a sampling device through over 150 m of water, it is conceivable that these two samples represent different depositional environments. Alternatively, the sample from this study is located near (within 200m) of the boundary of the depositional zone delineated by Thomas and Dell (1978). The lower sedimentation rate at the margin of this zone compared to a higher rate approximately 15 km to the center of the identified sub-basin could also be interpreted as validation of the zone delineation of Thomas and Dell (1978).

Core 2011-S008MC was collected at a standard U.S. EPA sampling location, and this location was sampled previously by Song et al. (2004). In that study, the sedimentation rate using the CRS model was reported as 0.0151 ± 0.0007 g/cm^2/y,

which is over twice the sedimentation rate determined in this study. Another nearby core is core L-142 from Kemp et al. (1978) which is approximately 15 km closer to the Keweenaw Peninsula, but measured to be only 13 m deeper in the same local basin as S008 from this study. The Kemp et al. (1978) pollen analysis yielded a sedimentation rate of 0.0025 g/cm^2/y, which is less than half of the result from this study. The sedimentation rate determined by this study falls in between the rates previously determined for this part of the lake.

Core 2011-S011MC is located in an area of the lake never previously sampled. However, core 25A from Kemp et al. (1978) is located approximately 27 km to the east, in a similar bathymetric setting. In that study, the sedimentation rate was found to be 0.0155 g/cm^2/y, which is considerably less than the value from this study, which is 0.0228 ± 0.0012 g/cm^2/y. This is most likely explained by the circulation patterns in the area, as S011 is located closer to Isle Royale, where one of the major gyres in Lake Superior flows to the south, and carries sediment from the northern shore and Nipigon Bay. The core from Kemp et al. (1978) is nearer the middle of the gyre, and less likely to be affected by sediment from Nipigon Bay.

Core 2011-S012MC is another standard EPA location that was sampled by Song et al. (2004). That study determined the sedimentation rate to be 0.0133 ± 0.0007 g/cm^2/y, which is slightly higher than the value determined in this study. Despite the fact that an attempt was made to sample at the same standard location, the coordinates reported place the samples 87 m apart, and the reported depths for the two samples are over 10 m different, suggesting that the actual sample locations

were not coincident and some variation in sedimentation rate is expected. Furthermore, other surrounding cores have values above and below the rates determined in this study and by Song et al. (2004). Examples include core 1383 from Kolak et al. (1998), which has recent sedimentation occurring at a rate of 0.0302 g/cm^2/y, while core 28 from Kemp et al. (1978) has a reported rate of 0.005 g/cm^2/y. Both of these examples are within approximately 35 km from S012 and have similar reported depths.

Core 2011-S016MC is another standard EPA location sampled by Song et al. (2004). In that study, this site was determined to have a sedimentation rate of 0.0111 ± 0.0003 g/cm^2/y, which is higher than the results of this study. However, less than 30 km from site S016 is the study location from Johnson et al. (2012). In that study, sedimentation rates were reported varying from 0.0049 g/cm^2/y to 0.0179 g/cm^2/y within only a few hundred meters horizontally. Therefore, even a few meters' variation spatially between Song et al. (2004) and the current study would explain the difference in sedimentation rate between those two cores.

Core 2011-S019MC is situated such that the nearest core, S-78 8BX from Evans et al. (1981) is not directly comparable, because it is a much shallower area on the margin of the Duluth sub-basin. Instead, comparison with other samples from a similar depth may be instructive, and the closest sample of a similar depth is core S78 4BX from Evans et al. (1981). This core is approximately 39 km to the southwest of S019, and is slightly shallower and closer to the shore. However, other cores in the vicinity are either very different in depth or have large slumping events

and influence of taconite tailing deposition. The S-78 4BX core, with a sedimentation rate of 0.016 g/cm^2/y, compares favorably with the results from this study if proximity to the major sediment supply from the nearby red clay bluffs is considered.

Core 2011-S022MC is located in an area of the lake with a high sampling density, and therefore comparison of the current study results to nearby previous results is comparatively straightforward. Furthermore, S022 is another standard EPA location that was sampled by Song et al. (2004). The reported sedimentation rate from Song et al. (2004) was 0.0151 ± 0.0007 g/cm^2/y, which is approximately one-half of the results of the current study. However, other nearby results indicate the Song et al. (2004) rate is anomalously low, as core S-78 1BX from Evans et al. (1981) reports a value of 0.045 g/cm^2/y, and core DTL was determined to have a sedimentation rate of 0.034 g/cm^2/y by Jeremiason (1993) and a rate in the range of 0.0202 g/cm^2/y to 0.0717 g/cm^2/y, all of which contain or exceed the rate in the current study.

Finally, core 2011-S114MC has a directly comparable result in the literature, due to its status as the deepest point in Lake Superior. Core DHC from Klump et al. (1989) is located approximately one kilometer from S114, in the same bathymetric depression. Klump et al. (1989) reported a sedimentation rate of $<<$0.030 g/cm^2/y, which is fully in agreement with the results of this study. Furthermore, the sedimentation rate derived in the current study adds a new level of quantification of sedimentation processes in the deepest basin of Lake Superior.

5.2. Comparison to Other Lakes

Lake Superior has been consistently reported in the literature as having the lowest average sedimentation rates among the Laurentian Great Lakes (e.g. Evans 1980). The rates in this study compare favorably to other Laurentian Great Lakes. The range of values for sedimentation rate determined in this study lies completely within the range of reported values for Lake Michigan (Fukumori et al. 1992) and Lake Huron (Robbins et al. 1977, Joshi 1985). The minimum value for sedimentation rate from this study is slightly below the lowest known rate in Lake Ontario (Kolak et al. 1998), but all values from this study are well below the highest rate in Lake Ontario (Rowan et al. 1995). Finally, all of the values from this study are well below the lowest rate reported for Lake Erie (Carter and Hites 1992).

5.3. Sediment Disturbance at Top of Cores

As previously mentioned, the initial absolute date results from all cores where a ^{137}Cs peak and/or the ^{241}Am onset are present indicated that some amount of sediment had been lost at some point before the top sample was obtained, or during the process of obtaining the core. In certain areas, regular re-suspension or scouring of the top layers of silty sediment has been identified as the primary cause of this missing sediment. This explanation fits at site S001, but is unlikely for any other core in this study. Another explanation for the loss of sediment is the development of a pressure wave ahead of the multi-corer as it is lowered to the bottom. Such a wave would be capable of displacing some sediment, especially a very low-density flocculent layer.

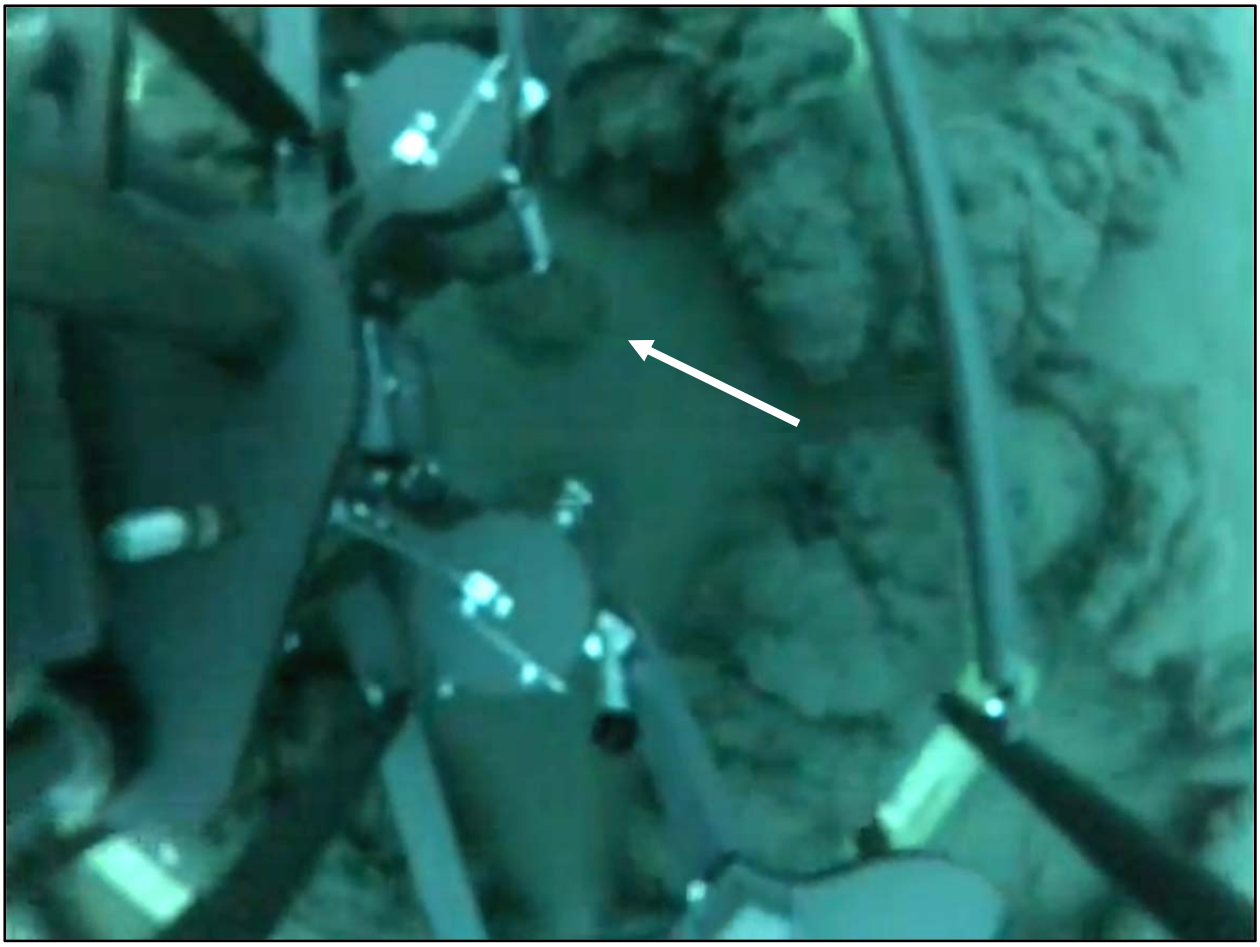

Figure 23. Photo of Multi-Corer Deployment Showing Sediment Disturbance

As shown in Figure 23, a certain amount of sediment is disturbed by the deployment of the Multi-Corer. This photo was taken using the same equipment as was used for the collection of the Lake Superior cores in 2011, but this photo was obtained from a video taken during the deployment of the device in Lake Huron in 2012. Some of the disturbed sediment is likely retained by the corer, but enough sediment may escape to justify the amount of sediment that would be required in order to align the ^{210}Pb-derived dates with the ^{137}Cs peak or ^{241}Am onset.

5.4. Focus Factors

The focus factors calculated for ^{210}Pb and ^{137}Cs are in many cases below unity, which should not be true of cores from depositional areas. These low values serve to validate the hypothesis that sediment is missing from the core, as this would cause the unsupported ^{210}Pb and the ^{137}Cs inventories to have an artificial deficiency. This appears to have occurred at sites S002, S008, S016, S019, and S114. Conversely, sites S011, S012, and S022 all have values near or above unity, indicating that most of the expected inventories are present, or sediment has moved from other parts of the lake to these sites. These observations of high focus factors strengthen the case for sediment movement in the Duluth sub-basin and from the northern marginal bays by the northern circulation gyre.

5.5. Updated Sedimentation Rate Map

The sedimentation rate map in Figure 22 is the first map of sedimentation rates for Lake Superior ever created using quantitative methods, and only the second such map ever published. This map, however, has many similarities to the map published by Evans (1980) in terms of general processes indicated by the map. In general, the highest sedimentation rates occur in the marginal bays of the lake, as well as in depositional areas immediately past natural current barriers such as the Keweenaw Peninsula and the end of the Duluth sub-basin. The areas of lowest sedimentation rates are the deepest parts that are furthest from the shore and sediment sources.

However, this map should be interpreted cautiously, because of the low sampling density in Lake Superior. Two main effects exist with so few features in the dataset. First, large parts of the lake remain unsampled, and so interpolation through these areas involves an assumption that the processes occurring at the sampled locations are the same as those in the areas with no sampling. The interpolation technique does not account for features such as bathymetry or current patterns explicitly and therefore may overgeneralize parts of the lake with few or no samples. Conversely, samples that are clustered in a small spatial area but with high variability in sedimentation values, such as in Whitefish Bay or at the survey area of Johnson et al. (2012), the interpolation technique may create patterns where one may not actually exist. The spline technique is an exact interpolator, which means that the resultant surface includes all of the data points exactly, which can result in exaggerated peaks and valleys, as seen in Whitefish Bay.

This map agrees well with descriptions of the sedimentation processes in the literature, as well as with the previously-published map. Applications for its use include discovery of under-sampled areas or areas that would benefit from more sampling to classify outliers, stronger visualization of trends compared to the previous method of only written descriptions, and as a framework for future efforts to compare results against, which will be especially useful in under-sampled areas.

6. Conclusions

Sedimentation rates determined in this study fall within the range of previously-reported values for Lake Superior, and validate the most recent sedimentation model for Lake Superior (Evans 1980). Indications of micro-scale differences in sedimentation, especially in the western half of the lake, as reported by Johnson et al. (2012) are also confirmed by comparison between data from this study and from Song et al. (2004).

Sediment core profiles indicate a loss of sediment at the surface of all cores, possibly implicating the sampling method as a source of this error. No definitive evidence for mixing of sediments is present in these cores, with a possible exception in the Duluth sub-basin. Six cores contained sufficient ^{137}Cs and/or ^{241}Am to calculate absolute dates for use as time control in studies of contaminant loading in these cores. Two cores, in the highly-complex eastern part of the lake, could not be calibrated to ^{241}Am onset data, suggesting conventional CRS and CIC models may not be well-suited for that environment.

Conversion of sample coordinates from previous studies to a common coordinate system exposed serious deficiencies in the description of the methods of spatial data collection, as well as documentation of the spatial coordinate system of reported locations, in those previous studies. These deficiencies required the development and utilization of a conversion framework based on the prevailing navigational technologies in use at the time of sampling.

Using the delineations of depositional areas by Thomas and Dell (1978), the data confirm deposition in all cores inside depositional areas, and non-deposition in cores outside of those areas. Furthermore, we observe very low sedimentation rates near the boundaries of these delineations. Sedimentation rate mapping in this study resembles the previous attempt, but incorporates twice the number of data points, and utilizes spline interpolation to generate rate contours.

CITED LITERATURE

Appleby, P.G., 2001. Chronostratigraphic Techniques in Recent Sediments. In: W.M. Last, J.P. Smol (Eds.), Tracking Environmental Change Using Lake Sediments. Volume 1: Basin Analysis, Coring, and Chronological Techniques. Kluwer Academic Publishers, Dordrecht, The Netherlands, pp. 171-202.

Basunia, M.S., 2006. Nuclear Data Sheets for A=237. Nuclear Data Sheets, 107, 2323–2422.

Bennett, E.B., 1978. Water Budgets for Lake Superior and Whitefish Bay. Journal of Great Lakes Research, 4(3-4), 331-342.

Bennington, V., McKinley, G.A., Kimura, N., Wu, C.H., 2010. General Circulation of Lake Superior: Mean, Variability, and Trends from 1979 to 2006. Journal of Geophysical Research, 115(C12).

Browne, E., 2003. Nuclear Data Sheets for A=210. Nuclear Data Sheets, 99, 483-753.

Browne, E., Tuli, J.K., 2007. Nuclear Data Sheets for A=137. Nuclear Data Sheets, 108, 2173-2318.

Bruland, K., Koide, M., Bowser, C., Maher, L.J., Goldberg, E.D., 1975. Lead-210 and Pollen Geochronologies on Lake Superior Sediments. Quaternary Research, 5, 89-98.

Carter, D.S., Hites, R.A., 1992. Fate and Transport of Detroit River Derived Pollutants throughout Lake Erie. Environmental Science and Technology, 26(7), 1333–1341.

Cartwright, J., Wattrus, N., Rausch, D., Bolton, A., 2004. Recognition of an early Holocene polygonal fault system in Lake Superior: Implications for the compaction of fine-grained sediments. Geology, 32(3), 253-256.

Evans, J.E., 1980. ^{210}Pb geochronology in Lake Superior sediments: Sedimentation rates, organic carbon deposition, sedimentary environments, and post-depositional processes. Master of Science, University of Minnesota, Minneapolis, 130 pp.

Evans, J.E., Johnson, T.C., Alexander, E.C.J., Lively, R.S., Eisenreich, S.J., 1981. Sedimentation Rates and Depositional Processes in Lake Superior from ^{210}Pb Geochronology. Journal of Great Lakes Research, 7(3), 299-310.

Fisher, A.J., 1996. A new technique for decoding Loran-C radionavigation signals. IEEE Transactions on Aerospace and Electronic Systems, 32(4), 1457-1467.

Flood, R.D., Johnson, T.C., 1984. Side-scan targets in Lake Superior - Evidence for bedforms and sediment transport. Sedimentology, 31, 311-333.

Frank, R.L., 1983. Current Developments in Loran-C. Proceedings of the IEEE, 71(3), 1127-1139.

Fukumori, E., Christensen, E.R., Klein, R.J., 1992. A model for ^{137}Cs and other tracers in lake sediments considering particle size and the inverse solution. Earth and Planetary Science Letters, 114(1), 85–99.

Hollenhorst, T.P., Johnson, L.B., Ciborowski, J., 2011. Monitoring land cover change in the Lake Superior basin. Aquatic Ecosystem Health & Management, 14(4), 433-442.

Jeremiason, J.D., 1993. Polychlorinated Biphenyls (PCBs) in Lake Superior, 1978-1992: Decreases in Water Concentrations Reflect Loss by Volatization. Master of Science, University of Minnesota, Minneapolis, 146 pp.

Johnson, T.C., Van Alstine, J.D., Rolfhus, K.R., Colman, S.M., Wattrus, N.J., 2012. A High Resolution Study of Spatial and Temporal Variability of Natural and Anthropogenic Compounds in Offshore Lake Superior Sediments. Journal of Great Lakes Research, 38, 673-685.

Joshi, S.R., 1985. Recent sedimentation rates and ^{210}Pb fluxes in Georgian Bay and Lake Huron. Science of the Total Environment, 41(3), 219–233.

Kemp, A.L.W., Dell, C.I., Harper, N.S., 1978. Sedimentation Rates and a Sediment Budget for Lake Superior. Journal of Great Lakes Research, 4(3-4), 276-287.

Klump, J.V., Paddock, R., Remsen, C.C., Fitzgerald, S., Boraas, M., Anderson, P., 1989. Variations in Sediment Accumulation Rates and the Flux of Labile Organic Matter in Eastern Lake Superior Basins. Journal of Great Lakes Research, 15(1), 104-122.

Kolak, J.J., Long, D.T., Beals, T.M., Eisenreich, S.J., Swackhamer, D.L., 1998. Anthropogenic Inventories and Historical and Present Accumulation Rates of Copper in Great Lakes Sediments. Applied Geochemistry, 13, 59-75.

Krishnaswamy, S., Lal, D., Martin, J.M., Meybeck, M., 1971. Geochronology of lake sediments. Earth and Planetary Science Letters, 11(1–5), 407-414.

Lenters, J.D., 2004. Trends in the Lake Superior Water Budget Since 1948: A Weakening Seasonal Cycle. Journal of Great Lakes Research, 30(Supplement 1), 20-40.

Maher, L.J., 1977. Palynological Studies in the Western Arm of Lake Superior. Quaternary Research, 7, 14-44.

Muir, D.C.G., Wang, X., Yang, F., Nguyen, N., Jackson, T.A., Evans, M.S., Douglas, M., Kock, G., Lamoureux, S., Pienitz, R., Smol, J.P., Vincent, W.F., Dastoor, A., 2009. Spatial Trends and Historical Deposition of Mercury in Eastern and Northern Canada Inferred from Lake Sediment Cores. Environmental Science and Technology, 43, 4802-4809.

Munawar, M., 1978. Some Common and Average Values for Lake Superior. Journal of Great Lakes Research, 4(3-4), 554.

Pearson, R.F., Swackhamer, D.L., Eisenreich, S.J., Long, D.T., 1997. Concentrations, Accumulations, and Inventories of Polychlorinated Dibenzo-*p*-dioxins and Dibenzofurans in Sediments of the Great Lakes. Environmental Science and Technology, 31, 2903-2909.

Quinn, F.H., 1992. Hydraulic residence times for the Laurentian Great Lakes. Journal of Great Lakes Research, 18(1), 22-28.

Radio Technical Commission for Marine Services. Special Committee, N., 1981. Minimum Performance Standards (MPS): Automatic Coordinate Conversion Systems, Radio Technical Commission for Marine Services, Washington, D.C.

Robbins, J.A., 1978. Geochemical and geophysical applications of radioactive lead. In: J.O. Nriagu (Ed.), The biogeochemistry of lead in the environment. Elsevier, Amsterdam, pp. 285-393.

Robbins, J.A., 1985. Great Lakes Regional Fallout Source Functions. In: G.L.E.R. Laboratory (Ed.). National Oceanic and Atmospheric Administration, Ann Arbor, Michigan.

Robbins, J.A., Edgington, D.N., 1975. Determination of recent sedimentation rates in Lake Michigan using Pb-210 and Cs-137. Geochimica et Cosmochimica Acta, 39, 285-304.

Robbins, J.A., Edgington, D.N., Kemp, A.L.W., 1978. Comparative ^{210}Pb, ^{137}Cs, and Pollen Geochronologies of Sediments from Lakes Ontario and Erie. Quaternary Research, 10, 256-278.

Robbins, J.A., Krezoski, J.R., Mozley, S.C., 1977. Radioactivity in sediments of the Great Lakes: Post-depositional redistribution by deposit-feeding organisms. Earth and Planetary Science Letters, 36(2), 325-333.

Rowan, D.J., Cornett, R.J., King, K., Risto, B., 1995. Sediment focusing and ^{210}Pb dating: a new approach. Journal of Paleolimnology, 13(2), 107-118.

Simcik, M.F., Eisenreich, S.J., Golden, K.A., Liu, S.-P., Lipiatou, E., Swackhamer, D.L., Long, D.T., 1996. Atmospheric Loading of Polycyclic Aromatic Hydrocarbons to Lake Michigan as Recorded in the Sediments. Environmental Science and Technology, 30(10), 3039–3046.

Simcik, M.F., Jeremiason, J.D., Lipiatou, E., Eisenreich, S.J., 2003. Enhanced Removal of Hydrophobic Organic Contaminants by Settling Sediments in Western Lake Superior. Journal of Great Lakes Research, 29(1), 41-53.

Singh, S., Jain, A.K., Tuli, J.K., 2011. Nuclear Data Sheets for A=222. Nuclear Data Sheets, 112, 2851-2886.

Song, W., Ford, J.C., Li, A., Mills, W.J., Buckley, D.R., Rockne, K.J., 2004. Polybrominated Diphenyl Ethers in the Sediments of the Great Lakes. 1. Lake Superior. Environmental Science and Technology, 38, 3286-3293.

Thomas, R.L., Dell, C.I., 1978. Sediments of Lake Superior. Journal of Great Lakes Research, 4(3-4), 264-275.

Williams, P., Last, D., 2003. On Loran-C Time-Difference to Co-ordinate Converters. In: M. Caruso (Ed.), 32nd Annual Convention & Technical Symposium of the International Loran Association. International Loran Association, Boulder, Colorado.

APPENDIX A

TABLE III. DATA FOR CORE 2011-S001MC

	Section Thick-ness (cm)	Avg. Depth (cm)	Dry Bulk Density (g/mL)	Decay-Adjusted Activity (Bq/kg)				CRS: ln(A0/Az)	CIC: ln(C0/Cx)	CRS: Adjusted Date (years)
				^{210}Pb	^{226}Ra	^{137}Cs	^{241}Am			
S001MC-01	0.5	0.25	1.213	177 ± 5	8.8 ± 2.4	22 ± 1	≤ 0.5			
S001MC-02	0.5	0.75	1.206	57 ± 6	9.2 ± 3.1	19 ± 1	≤ 0.7			
S001MC-03	0.5	1.25	1.109	15 ± 5	12 ± 4	2.1 ± 0.4	≤ 0.7			
S001MC-04	0.5	1.75	1.190	10 ± 3	19 ± 2	≤ 0.4	≤ 0.4			
S001MC-05	0.5	2.25	1.138	22 ± 6	17 ± 4	≤ 0.7	≤ 0.7			
S001MC-06	0.5	2.75	1.074	23 ± 7	21 ± 4	≤ 0.8	≤ 0.8			
S001MC-07	0.5	3.25	1.140	20 ± 6	14 ± 4	≤ 0.7	≤ 0.7			
S001MC-08	0.5	3.75	1.125	12 ± 5	19 ± 4	≤ 0.8	≤ 0.7			
S001MC-09	0.5	4.25	1.024	25 ± 3	23 ± 3	≤ 0.4	≤ 0.4			
S001MC-10	0.5	4.75	1.024	20 ± 3	18 ± 3	≤ 0.5	≤ 0.5			
S001MC-11	1	5.5	1.097	21 ± 5	23 ± 4	≤ 0.7	≤ 0.7			
S001MC-12	1	6.5	1.071	25 ± 3	26 ± 3	≤ 0.5	≤ 0.4			
S001MC-13	1	7.5	1.190	24 ± 5	20 ± 4	≤ 0.8	≤ 0.7			
S001MC-14	1	8.5	0.923	34 ± 6	30 ± 5	≤ 0.9	≤ 0.7			
S001MC-15	1	9.5	1.189	38 ± 4	29 ± 3	≤ 0.6	≤ 0.5			
S001MC-16	1	10.5	0.869	39 ± 6	27 ± 4	≤ 0.8	≤ 0.7			
S001MC-17	1	11.5	0.870	39 ± 3	33 ± 2	≤ 0.4	≤ 0.4			
S001MC-18	1	12.5	0.958	46 ± 6	33 ± 3	≤ 0.6	≤ 0.5			
S001MC-19	1	13.5	0.906	43 ± 4	32 ± 3	≤ 0.5	≤ 0.4			
S001MC-20	1	14.5	0.844	47 ± 5	35 ± 4	≤ 0.7	≤ 0.6			
S001MC-21	2	16	0.732	38 ± 5	38 ± 4	≤ 0.7	≤ 0.6			
S001MC-22	2	18	0.834	39 ± 6	34 ± 5	≤ 0.9	≤ 0.7			
S001MC-23	2	20	0.771	46 ± 5	40 ± 4	≤ 0.7	≤ 0.5			
S001MC-24	2	22	0.536	58 ± 8	48 ± 5	≤ 1.0	≤ 0.8			

CRS Sedimentation Rate:
CIC Sedimentation Rate:
^{210}Pb Focus Factor:
^{137}Cs Focus Factor:
Lost Sediment Thickness:
Lost Sediment Dry Bulk Density:
Lost Sediment Average Date:

TABLE IV. DATA FOR CORE 2011-S002MC

	Section Thick-ness (cm)	Avg. Depth (cm)	Dry Bulk Density (g/mL)	Decay-Adjusted Activity (Bq/kg)				CRS: ln(A0/Az)	CIC: ln(C0/Cx)	CRS: Adjusted Date (years)
				^{210}Pb	^{226}Ra	^{137}Cs	^{241}Am			
S002MC-01	0.5	0.25	0.107	2197 ± 25	37 ± 8	261 ± 3	5.1 ± 0.9	0.000	0.000	1983
S002MC-02	0.5	0.75	0.241	1529 ± 18	48 ± 7	231 ± 3	3.9 ± 0.6	0.270	0.377	1972
S002MC-03	0.5	1.25	0.330	752 ± 13	38 ± 5	181 ± 2	2.8 ± 0.5	0.921	1.107	1954
S002MC-04	0.5	1.75	0.435	255 ± 7	33 ± 3	86 ± 1	≤ 0.6	1.852	2.276	1930
S002MC-05	0.5	2.25	0.557	100 ± 8	25 ± 4	26 ± 1	≤ 0.7	2.845	3.352	1899
S002MC-06	0.5	2.75	0.628	47 ± 4	24 ± 3	9.6 ± 0.5	≤ 0.5	4.194	4.522	1862
S002MC-07	0.5	3.25	0.556	45 ± 6	40 ± 5	3.0 ± 0.5	≤ 0.7			1825
S002MC-08	0.5	3.75	0.501	52 ± 7	36 ± 4	3.4 ± 0.6	≤ 0.8			1792
S002MC-09	0.5	4.25	0.512	46 ± 4	33 ± 3	2.1 ± 0.4	≤ 0.5			1761
S002MC-10	0.5	4.75	0.570	32 ± 5	34 ± 4	1.2 ± 0.4	≤ 0.7			1727
S002MC-11	1	5.5	0.797	30 ± 6	35 ± 4	≤ 0.7	≤ 0.7			1660
S002MC-12	1	6.5	0.592	39 ± 8	46 ± 5	≤ 1.0	≤ 0.9			1573
S002MC-13	1	7.5	0.547	54 ± 4	50 ± 3	≤ 0.5	≤ 0.5			1502
S002MC-14	1	8.5	0.541	50 ± 5	42 ± 3	≤ 0.5	≤ 0.5			1435
S002MC-15	1	9.5	0.548	53 ± 3	42 ± 3	≤ 0.4	≤ 0.4			1367
S002MC-16	1	10.5	0.573	45 ± 8	50 ± 6	≤ 1.0	≤ 0.9			1297
S002MC-17	1	11.5	0.564	51 ± 8	39 ± 5	≤ 0.9	≤ 0.9			1226
S002MC-18	1	12.5	0.587	42 ± 6	50 ± 6	≤ 0.9	≤ 1.0			1154
S002MC-19	1	13.5	0.592	42 ± 7	47 ± 5	≤ 0.9	≤ 1.0			1081
S002MC-20	1	14.5	0.596	50 ± 5	36 ± 4	≤ 0.7	≤ 0.7			1007
S002MC-21	2	16	0.582	58 ± 7	45 ± 5	≤ 0.8	≤ 0.9			897
S002MC-22	2	18	0.604	56 ± 6	46 ± 4	≤ 0.7	≤ 0.8			750
S002MC-23	2	20	0.595	54 ± 5	44 ± 4	≤ 0.6	≤ 0.7			600
S002MC-24	2	22	0.601	42 ± 5	52 ± 4	≤ 0.7	≤ 0.7			451
S002MC-25	2	24	0.597	49 ± 6	45 ± 4	≤ 0.7	≤ 0.7			302

				Lost Sediment Thickness	≈ 1.9 cm
CRS Sedimentation Rate:	0.0080 ± 0.0002 g/cm²/y	^{210}Pb Focus Factor:	0.85	Lost Sediment Dry Bulk Density	≈ 0.107 g/mL
CIC Sedimentation Rate:	0.0073 ± 0.0002 g/cm²/y	^{137}Cs Focus Factor:		Lost Sediment Average Date	≈ 1999

TABLE V. DATA FOR CORE 2011-S008MC

	Section Thick-ness (cm)	Avg. Depth (cm)	Dry Bulk Density (g/mL)	Decay-Adjusted Activity (Bq/kg)				CRS: ln(A0/Az)	CIC: ln(C0/Cx)	CRS: Adjusted Date (years)
				^{210}Pb	^{226}Ra	^{137}Cs	^{241}Am			
S008MC-01	0.5	0.25	0.145	1792 ± 24	50 ± 8	342 ± 4	8.0 ± 1.1	0.000	0.000	
S008MC-02	0.5	0.75	0.163	1391 ± 15	46 ± 6	299 ± 3	5.7 ± 0.8	0.341	0.259	
S008MC-03	0.5	1.25	0.198	819 ± 9	51 ± 5	226 ± 2	3.8 ± 0.5	0.777	0.820	
S008MC-04	0.5	1.75	0.229	483 ± 14	44 ± 8	184 ± 3	4.4 ± 1.0	1.252	1.379	
S008MC-05	0.5	2.25	0.250	337 ± 8	57 ± 5	137 ± 2	3.1 ± 0.5	1.769	1.827	
S008MC-06	0.5	2.75	0.276	204 ± 6	57 ± 5	54 ± 1	1.4 ± 0.4	2.405	2.474	
S008MC-07	0.5	3.25	0.316	126 ± 9	52 ± 6	13 ± 1	≤ 1.2	3.125	3.154	
S008MC-08	0.5	3.75	0.329	92 ± 8	47 ± 7	3.8 ± 0.8	≤ 1.1	4.075	3.655	
S008MC-09	0.5	4.25	0.392	48 ± 8	44 ± 7	≤ 1.1	≤ 1.1			
S008MC-10	0.5	4.75	0.399	65 ± 9	53 ± 7	≤ 1.1	≤ 1.2			
S008MC-11	1	5.5	0.439	46 ± 6	60 ± 5	≤ 0.7	≤ 0.8			
S008MC-12	1	6.5	0.490	52 ± 4	38 ± 4	≤ 0.5	≤ 0.6			
S008MC-13	1	7.5	0.484	53 ± 8	43 ± 7	≤ 1.0	≤ 1.1			
S008MC-14	1	8.5	0.490	56 ± 8	53 ± 7	≤ 1.0	≤ 1.1			
S008MC-15	1	9.5	0.526	56 ± 6	40 ± 4	≤ 0.6	≤ 0.7			
S008MC-16	1	10.5	0.527	53 ± 8	46 ± 5	≤ 0.9	≤ 1.0			
S008MC-17	1	11.5	0.529	44 ± 8	42 ± 7	≤ 1.1	≤ 1.2			
S008MC-18	1	12.5	0.540	60 ± 8	39 ± 6	≤ 0.9	≤ 1.0			
S008MC-19	1	13.5	0.552	48 ± 7	39 ± 6	≤ 1.0	≤ 1.1			
S008MC-20	1	14.5	0.561	40 ± 7	47 ± 7	≤ 1.1	≤ 1.2			
S008MC-21	2	16	0.565	44 ± 8	37 ± 6	≤ 0.9	≤ 1.0			
S008MC-22	2	18	0.605	53 ± 8	30 ± 6	≤ 1.0	≤ 1.1			
S008MC-23	2	20	0.630	52 ± 7	40 ± 5	≤ 1.0	≤ 1.0			
S008MC-24	2	22	0.698	44 ± 7	33 ± 6	≤ 1.0	≤ 1.0			
S008MC-25	2	24	0.642	47 ± 5	44 ± 4	≤ 0.6	≤ 0.6			

				Lost Sediment Thickness:
CRS Sedimentation Rate:	0.0069 ± 0.0001 g/cm²/y	^{210}Pb Focus Factor:	0.76	Lost Sediment Dry Bulk Density:
CIC Sedimentation Rate:	0.0073 ± 0.0002 g/cm²/y	^{137}Cs Focus Factor:		Lost Sediment Average Date:

TABLE VI. DATA FOR CORE 2011-S011MC

	Section Thick-ness (cm)	Avg. Depth (cm)	Dry Bulk Density (g/mL)	Decay-Adjusted Activity (Bq/kg)				CRS: ln(A0/Az)	CIC: ln(C0/Cx)	CRS: Adjusted Date (years)
				^{210}Pb	^{226}Ra	^{137}Cs	^{241}Am			
S011MC-01	0.5	0.25	0.162	1975 ± 25	58 ± 10	232 ± 3	4.8 ± 0.9	0.000	0.000	2009
S011MC-02	0.5	0.75	0.176	1851 ± 25	56 ± 8	250 ± 3	4.0 ± 0.9	0.172	0.065	2005
S011MC-03	0.5	1.25	0.191	1517 ± 14	50 ± 5	292 ± 2	3.9 ± 0.6	0.383	0.267	2001
S011MC-04	0.5	1.75	0.221	1253 ± 18	36 ± 6	333 ± 3	6.3 ± 0.9	0.618	0.454	1996
S011MC-05	0.5	2.25	0.239	978 ± 16	61 ± 7	387 ± 3	7.6 ± 0.8	0.909	0.737	1991
S011MC-06	0.5	2.75	0.261	715 ± 14	45 ± 6	287 ± 3	5.3 ± 0.8	1.232	1.051	1986
S011MC-07	0.5	3.25	0.332	367 ± 6	46 ± 4	120 ± 1	2.0 ± 0.4	1.595	1.786	1979
S011MC-08	0.5	3.75	0.365	228 ± 10	41 ± 6	77 ± 2	2.2 ± 0.7	1.904	2.328	1972
S011MC-09	0.5	4.25	0.415	186 ± 6	49 ± 4	64 ± 1	1.4 ± 0.4	2.169	2.639	1963
S011MC-10	0.5	4.75	0.440	141 ± 8	36 ± 5	49 ± 1	1.8 ± 0.5	2.459	2.905	1954
S011MC-11	1	5.5	0.522	86 ± 9	37 ± 6	13 ± 1	≤ 1.0	2.779	3.658	1938
S011MC-12	1	6.5	0.512	71 ± 7	31 ± 5	1.1 ± 0.4	≤ 0.8	3.328	3.856	1915
S011MC-13	1	7.5	0.575	52 ± 6	41 ± 6	≤ 0.7	≤ 0.9	4.214	5.215	1891
S011MC-14	1	8.5	0.549	52 ± 7	36 ± 5	≤ 0.7	≤ 0.8	4.743	4.808	1867
S011MC-15	1	9.5	0.558	42 ± 6	47 ± 6	≤ 0.7	≤ 0.8			1843
S011MC-16	1	10.5	0.585	37 ± 7	44 ± 6	≤ 0.7	≤ 0.8			1818
S011MC-17	1	11.5	0.617	44 ± 3	35 ± 3	≤ 0.4	≤ 0.5			1791
S011MC-18	1	12.5	0.665	43 ± 6	37 ± 5	≤ 0.7	≤ 0.8			1763
S011MC-19	1	13.5	0.658	45 ± 4	35 ± 3	≤ 0.4	≤ 0.5			1734
S011MC-20	1	14.5	0.610	47 ± 5	40 ± 4	≤ 0.5	≤ 0.6			1706
S011MC-21	2	16	0.644	39 ± 6	34 ± 5	≤ 0.7	≤ 0.8			1665
S011MC-22	2	18	0.606	52 ± 7	44 ± 5	≤ 0.7	≤ 0.8			1610
S011MC-23	2	20	0.573	43 ± 5	35 ± 4	≤ 0.4	≤ 0.5			1559
S011MC-24	2	22	0.611	41 ± 6	48 ± 5	≤ 0.6	≤ 0.8			1507
S011MC-25	2	24	0.598	37 ± 6	28 ± 4	≤ 0.6	≤ 0.8			1454

				Lost Sediment Thickness:	≈ 0.1 cm
CRS Sedimentation Rate:	0.0228 ± 0.0012 g/cm²/y	^{210}Pb Focus Factor:	1.72	Lost Sediment Dry Bulk Density:	≈ 0.162 g/mL
CIC Sedimentation Rate:	0.0187 ± 0.0015 g/cm²/y	^{137}Cs Focus Factor:	1.21	Lost Sediment Average Date:	≈ 2011

TABLE VII. DATA FOR CORE 2011-S012MC

	Section Thick-ness (cm)	Avg. Depth (cm)	Dry Bulk Density (g/mL)	Decay-Adjusted Activity (Bq/kg)				CRS: ln(A0/Az)	CIC: ln(C0/Cx)	CRS: Adjusted Date (years)
				^{210}Pb	^{226}Ra	^{137}Cs	^{241}Am			
S012MC-01	0.5	0.25	0.150	1974 ± 15	55 ± 6	266 ± 2	3.5 ± 0.6	0.000	0.000	1991
S012MC-02	0.5	0.75	0.172	1664 ± 16	46 ± 6	289 ± 3	4.5 ± 0.7	0.201	0.170	1982
S012MC-03	0.5	1.25	0.186	1472 ± 22	58 ± 10	346 ± 4	5.4 ± 1.0	0.444	0.305	1973
S012MC-04	0.5	1.75	0.195	1109 ± 17	49 ± 8	393 ± 4	6.2 ± 0.7	0.745	0.593	1963
S012MC-05	0.5	2.25	0.219	884 ± 11	49 ± 5	346 ± 2	6.5 ± 0.6	1.069	0.832	1952
S012MC-06	0.5	2.75	0.235	623 ± 15	53 ± 9	269 ± 3	5.7 ± 0.9	1.479	1.214	1940
S012MC-07	0.5	3.25	0.251	417 ± 13	54 ± 9	137 ± 2	2.7 ± 0.9	1.945	1.664	1928
S012MC-08	0.5	3.75	0.268	274 ± 12	46 ± 9	34 ± 2	1.6 ± 0.7	2.461	2.131	1914
S012MC-09	0.5	4.25	0.280	148 ± 11	54 ± 8	7.9 ± 1.0	≤ 1.2	3.067	3.012	1900
S012MC-10	0.5	4.75	0.295	113 ± 6	43 ± 4	2.4 ± 0.4	≤ 0.7	3.513	3.318	1885
S012MC-11	1	5.5	0.300	92 ± 8	61 ± 7	≤ 1.0	≤ 1.4	4.085	4.110	1862
S012MC-12	1	6.5	0.326	64 ± 10	52 ± 7	≤ 1.1	≤ 0.7	5.325	5.093	1829
S012MC-13	1	7.5	0.330	72 ± 9	52 ± 7	≤ 1.0	≤ 1.1			1795
S012MC-14	1	8.5	0.351	58 ± 5	50 ± 4	≤ 0.6	≤ 0.6			1759
S012MC-15	1	9.5	0.363	65 ± 6	48 ± 4	≤ 0.7	≤ 0.8			1722
S012MC-16	1	10.5	0.377	51 ± 8	51 ± 7	≤ 1.0	≤ 1.1			1683
S012MC-17	1	11.5	0.386	51 ± 8	44 ± 8	≤ 1.0	≤ 1.1			1644
S012MC-18	1	12.5	0.393	49 ± 5	44 ± 4	≤ 0.6	≤ 0.7			1603
S012MC-19	1	13.5	0.387	55 ± 8	53 ± 7	≤ 1.1	≤ 1.1			1562
S012MC-20	1	14.5	0.387	69 ± 11	48 ± 8	≤ 1.1	≤ 1.3			1522
S012MC-21	2	16	0.380	60 ± 8	51 ± 6	≤ 1.0	≤ 1.0			1462
S012MC-22	2	18	0.379	50 ± 9	37 ± 7	≤ 1.1	≤ 1.3			1383
S012MC-23	2	20	0.390	52 ± 6	48 ± 4	≤ 0.6	≤ 0.6			1303
S012MC-24	2	22	0.405	50 ± 8	51 ± 6	≤ 0.9	≤ 1.0			1220
S012MC-25	2	24	0.410	54 ± 9	45 ± 7	≤ 1.1	≤ 1.2			1135
S012MC-26	2	41	0.388	47 ± 8	44 ± 6	≤ 1.0	≤ 1.1			1052

				Lost Sediment Thickness:	≈ 1.3 cm
CRS Sedimentation Rate:	0.0096 ± 0.0002 g/cm²/y	^{210}Pb Focus Factor:	1.38	Lost Sediment Dry Bulk Density:	≈ 0.123 g/mL
CIC Sedimentation Rate:	0.0096 ± 0.0003 g/cm²/y	^{137}Cs Focus Factor:	0.99	Lost Sediment Average Date:	≈ 2003

TABLE VIII. DATA FOR CORE 2011-S016MC

	Section Thick-ness (cm)	Avg. Depth (cm)	Dry Bulk Density (g/mL)	Decay-Adjusted Activity (Bq/kg)				CRS: ln(A0/Az)	CIC: ln(C0/Cx)	CRS: Adjusted Date (years)
				^{210}Pb	^{226}Ra	^{137}Cs	^{241}Am			
S016MC-01	0.5	0.25	0.142	1685 ± 14	38 ± 5	272 ± 2	4.8 ± 0.7	0.000	0.000	1996
S016MC-02	0.5	0.75	0.180	1349 ± 17	54 ± 6	259 ± 3	5.0 ± 0.7	0.220	0.240	1987
S016MC-03	0.5	1.25	0.204	1084 ± 19	40 ± 8	238 ± 3	2.9 ± 0.9	0.500	0.456	1976
S016MC-04	0.5	1.75	0.223	903 ± 17	45 ± 6	250 ± 3	4.4 ± 1.0	0.852	0.652	1963
S016MC-05	0.5	2.25	0.298	606 ± 13	38 ± 6	211 ± 2	3.3 ± 0.7	1.327	1.065	1948
S016MC-06	0.5	2.75	0.366	252 ± 7	44 ± 3	102 ± 1	3.1 ± 0.5	2.099	2.068	1928
S016MC-07	0.5	3.25	0.484	143 ± 9	41 ± 7	53 ± 1	2.5 ± 0.8	2.842	2.782	1903
S016MC-08	0.5	3.75	0.488	68 ± 8	45 ± 5	18 ± 1	≤ 1.2	4.092	4.250	1874
S016MC-09	0.5	4.25	0.525	49 ± 8	33 ± 7	2.1 ± 0.7	2.6 ± 0.8	4.957	4.643	1845
S016MC-10	0.5	4.75	0.565	45 ± 4	40 ± 4	≤ 0.5	1.1 ± 0.4			1812
S016MC-11	1	5.5	0.567	51 ± 8	40 ± 6	≤ 1.0	≤ 1.5			1762
S016MC-12	1	6.5	0.531	41 ± 7	45 ± 7	≤ 1.0	≤ 1.4			1698
S016MC-13	1	7.5	0.536	52 ± 8	44 ± 6	≤ 0.9	≤ 1.0			1635
S016MC-14	1	8.5	0.559	54 ± 10	47 ± 8	≤ 1.0	≤ 1.5			1570
S016MC-15	1	9.5	0.562	53 ± 5	47 ± 4	≤ 0.6	≤ 0.8			1504
S016MC-16	1	10.5	0.559	50 ± 8	39 ± 6	≤ 1.0	≤ 1.2			1438
S016MC-17	1	11.5	0.535	40 ± 8	41 ± 6	≤ 1.0	≤ 1.2			1374
S016MC-18	1	12.5	0.600	45 ± 7	42 ± 6	≤ 0.9	≤ 1.5			1307
S016MC-19	1	13.5	0.567	48 ± 8	56 ± 7	≤ 1.0	≤ 1.4			1238
S016MC-20	1	14.5	0.572	53 ± 9	43 ± 6	≤ 1.0	≤ 1.4			1171
S016MC-21	2	16	0.567	45 ± 6	49 ± 5	≤ 0.8	≤ 1.0			1071
S016MC-22	2	18	0.580	56 ± 8	46 ± 7	≤ 0.9	≤ 1.3			936
S016MC-23	2	20	0.554	51 ± 8	49 ± 6	≤ 0.9	≤ 1.4			802
S016MC-24	2	22	0.551	46 ± 7	41 ± 5	≤ 0.9	≤ 1.3			672
S016MC-25	2	24	0.578	45 ± 7	43 ± 6	≤ 0.9	≤ 1.2			539

				Lost Sediment Thickness:	≈ 0.9 cm
CRS Sedimentation Rate:	0.0085 ± 0.0002 g/cm²/y	^{210}Pb Focus Factor:	1.03	Lost Sediment Dry Bulk Density:	≈ 0.109 g/mL
CIC Sedimentation Rate:	0.0085 ± 0.0004 g/cm²/y	^{137}Cs Focus Factor:	0.77	Lost Sediment Average Date:	≈ 2006

TABLE IX. DATA FOR CORE 2011-S019MC

	Section Thick-ness (cm)	Avg. Depth (cm)	Dry Bulk Density (g/mL)	Decay-Adjusted Activity (Bq/kg)				CRS: ln(A0/Az)	CIC: ln(C0/Cx)	CRS: Adjusted Date (years)
				^{210}Pb	^{226}Ra	^{137}Cs	^{241}Am			
S019MC-01	0.5	0.25	0.214	1258 ± 12	30 ± 5	181 ± 2	2.0 ± 0.6	0.000	0.000	1985
S019MC-02	0.5	0.75	0.242	919 ± 18	35 ± 8	194 ± 3	5.6 ± 1.0	0.325	0.329	1975
S019MC-03	0.5	1.25	0.290	518 ± 15	32 ± 8	196 ± 3	5.1 ± 0.7	0.701	0.927	1963
S019MC-04	0.5	1.75	0.287	421 ± 10	36 ± 6	167 ± 2	4.8 ± 0.7	1.059	1.160	1950
S019MC-05	0.5	2.25	0.260	354 ± 8	42 ± 5	91 ± 1	2.9 ± 0.6	1.470	1.370	1938
S019MC-06	0.5	2.75	0.268	243 ± 8	46 ± 5	17 ± 1	≤ 1.0	1.937	1.831	1926
S019MC-07	0.5	3.25	0.275	177 ± 12	47 ± 6	2.6 ± 0.8	≤ 1.3	2.426	2.251	1914
S019MC-08	0.5	3.75	0.280	103 ± 11	54 ± 8	≤ 1.2	≤ 1.4	2.980	3.225	1901
S019MC-09	0.5	4.25	0.288	84 ± 7	51 ± 4	≤ 0.6	≤ 0.7	3.314	3.637	1889
S019MC-10	0.5	4.75	0.300	60 ± 8	49 ± 7	≤ 1.0	≤ 1.0	3.630	4.747	1875
S019MC-11	1	5.5	0.325	68 ± 10	34 ± 5	≤ 1.0	≤ 1.2	3.766	3.596	1854
S019MC-12	1	6.5	0.309	58 ± 9	57 ± 8	≤ 1.0	≤ 1.1			1826
S019MC-13	1	7.5	0.342	53 ± 8	49 ± 7	≤ 1.0	≤ 1.1			1797
S019MC-14	1	8.5	0.357	55 ± 5	53 ± 4	≤ 0.6	≤ 0.6			1765
S019MC-15	1	9.5	0.360	51 ± 6	46 ± 5	≤ 0.7	≤ 0.7			1733
S019MC-16	1	10.5	0.358	38 ± 8	58 ± 6	≤ 0.9	≤ 1.0			1701
S019MC-17	1	11.5	0.363	55 ± 5	49 ± 4	≤ 0.6	≤ 0.6			1668
S019MC-18	1	12.5	0.380	47 ± 8	40 ± 6	≤ 0.9	≤ 1.0			1635
S019MC-19	1	13.5	0.415	36 ± 8	44 ± 8	≤ 1.5	≤ 1.4			1599
S019MC-20	1	14.5	0.430	43 ± 6	39 ± 4	≤ 0.7	≤ 0.8			1562
S019MC-21	2	16	0.450	52 ± 7	47 ± 5	≤ 0.9	≤ 1.0			1502
S019MC-22	2	18	0.469	51 ± 4	47 ± 3	≤ 0.5	≤ 0.5			1420
S019MC-23	2	20	0.469	65 ± 7	65 ± 6	≤ 0.8	≤ 0.8			1335
S019MC-24	2	22	0.437	59 ± 5	43 ± 3	≤ 0.5	≤ 0.6			1254
S019MC-25	2	24	0.408	40 ± 5	59 ± 5	≤ 0.7	≤ 0.7			1179

				Lost Sediment Thickness:	≈ 1.1 cm
CRS Sedimentation Rate:	0.0111 ± 0.0007 g/cm²/y	^{210}Pb Focus Factor:	0.82	Lost Sediment Dry Bulk Density:	≈ 0.214 g/mL
CIC Sedimentation Rate:	0.0094 ± 0.0011 g/cm²/y	^{137}Cs Focus Factor:	0.52	Lost Sediment Average Date:	≈ 2001

TABLE X. DATA FOR CORE 2011-S022MC

	Section Thick-ness (cm)	Avg. Depth (cm)	Dry Bulk Density (g/mL)	Decay-Adjusted Activity (Bq/kg)				CRS: ln(A0/Az)	CIC: ln(C0/Cx)	CRS: Adjusted Date (years)
				^{210}Pb	^{226}Ra	^{137}Cs	^{241}Am			
S022MC-01	0.5	0.25	0.250	631 ± 13	51 ± 6	98 ± 2	≤ 1.0	0.000	0.000	1988
S022MC-02	0.5	0.75	0.272	668 ± 13	58 ± 6	105 ± 2	≤ 0.9	0.138	-0.050	1984
S022MC-03	0.5	1.25	0.303	582 ± 8	56 ± 4	117 ± 1	0.8 ± 0.4	0.323	0.096	1979
S022MC-04	0.5	1.75	0.346	434 ± 11	40 ± 5	141 ± 2	2.2 ± 0.6	0.541	0.389	1974
S022MC-05	0.5	2.25	0.378	295 ± 8	47 ± 5	176 ± 2	2.4 ± 0.5	0.773	0.850	1969
S022MC-06	0.5	2.75	0.400	213 ± 7	57 ± 4	178 ± 2	4.2 ± 0.5	0.972	1.312	1963
S022MC-07	0.5	3.25	0.390	170 ± 9	44 ± 6	140 ± 2	3.8 ± 0.7	1.130	1.527	1957
S022MC-08	0.5	3.75	0.387	177 ± 10	46 ± 6	80 ± 2	≤ 1.1	1.275	1.485	1951
S022MC-09	0.5	4.25	0.385	148 ± 9	48 ± 6	43 ± 1	≤ 1.0	1.451	1.762	1945
S022MC-10	0.5	4.75	0.392	134 ± 9	63 ± 7	12 ± 1	≤ 0.9	1.608	2.112	1939
S022MC-11	1	5.5	0.406	129 ± 8	55 ± 6	2.2 ± 0.6	≤ 0.9	1.738	2.050	1930
S022MC-12	1	6.5	0.417	95 ± 5	51 ± 4	≤ 0.4	≤ 0.5	2.103	2.570	1918
S022MC-13	1	7.5	0.423	86 ± 7	50 ± 6	≤ 0.7	≤ 0.9	2.416	2.790	1905
S022MC-14	1	8.5	0.388	87 ± 7	54 ± 5	≤ 0.8	≤ 0.9	2.771	2.866	1893
S022MC-15	1	9.5	0.383	76 ± 9	51 ± 6	≤ 0.8	≤ 0.9	3.223	3.129	1881
S022MC-16	1	10.5	0.386	71 ± 7	51 ± 6	≤ 0.7	≤ 0.9	3.792	3.358	1869
S022MC-17	1	11.5	0.399	60 ± 7	48 ± 6	≤ 0.7	≤ 0.9	4.741	3.852	1858
S022MC-18	1	12.5	0.407	52 ± 6	51 ± 5	≤ 0.6	≤ 0.7			1845
S022MC-19	1	13.5	0.394	57 ± 7	50 ± 6	≤ 0.8	≤ 0.9			1833
S022MC-20	1	14.5	0.378	62 ± 7	54 ± 6	≤ 0.8	≤ 0.9			1822
S022MC-21	2	16	0.376	51 ± 5	49 ± 3	≤ 0.4	≤ 0.5			1804
S022MC-22	2	18	0.396	63 ± 8	40 ± 5	≤ 0.7	≤ 0.8			1781
S022MC-23	2	20	0.398	73 ± 10	54 ± 6	≤ 0.7	≤ 1.0			1757
S022MC-24	2	22	0.405	55 ± 5	52 ± 4	≤ 0.5	≤ 0.6			1733
S022MC-25	2	24	0.422	49 ± 4	50 ± 3	≤ 0.4	≤ 0.5			1708

				Lost Sediment Thickness:	≈ 2.9 cm
CRS Sedimentation Rate:	0.0330 ± 0.0014 g/cm²/y	^{210}Pb Focus Factor:	0.98	Lost Sediment Dry Bulk Density:	≈ 0.251 g/mL
CIC Sedimentation Rate:	0.0352 ± 0.0022 g/cm²/y	^{137}Cs Focus Factor:	0.91	Lost Sediment Average Date:	≈ 2000

TABLE XI. DATA FOR CORE 2011-S114MC

	Section Thick-ness (cm)	Avg. Depth (cm)	Dry Bulk Density (g/mL)	Decay-Adjusted Activity (Bq/kg)				CRS: ln(A0/Az)	CIC: ln(C0/Cx)	CRS: Adjusted Date (years)
				^{210}Pb	^{226}Ra	^{137}Cs	^{241}Am			
S114MC-01	0.5	0.25	0.431	808 ± 11	18 ± 4	86 ± 1	0.9 ± 0.4	0.000	0.000	
S114MC-02	0.5	0.75	0.649	477 ± 11	22 ± 5	72 ± 2	1.2 ± 0.5	0.590	0.552	
S114MC-03	0.5	1.25	0.570	206 ± 6	23 ± 4	40 ± 1	0.7 ± 0.3	1.784	1.464	
S114MC-04	0.5	1.75	0.525	66 ± 7	20 ± 5	15 ± 1	≤ 0.9	3.457	2.845	
S114MC-05	0.5	2.25	0.674	33 ± 8	36 ± 5	2.3 ± 0.6	≤ 0.9			
S114MC-06	0.5	2.75	0.729	38 ± 8	36 ± 6	≤ 0.9	≤ 1.0			
S114MC-07	0.5	3.25	0.751	41 ± 7	30 ± 5	≤ 0.8	≤ 0.8			
S114MC-08	0.5	3.75	0.740	33 ± 6	38 ± 6	≤ 0.9	≤ 1.0			
S114MC-09	0.5	4.25	0.644	42 ± 6	39 ± 4	≤ 0.6	≤ 0.7			
S114MC-10	0.5	4.75	0.639	44 ± 7	40 ± 5	≤ 0.8	≤ 0.9			
S114MC-11	1	5.5	0.663	38 ± 5	36 ± 4	≤ 0.6	≤ 0.7			
S114MC-12	1	6.5	0.788	33 ± 7	30 ± 5	≤ 0.8	≤ 0.8			
S114MC-13	1	7.5	0.827	25 ± 7	29 ± 5	≤ 0.8	≤ 0.9			
S114MC-14	1	8.5	0.802	37 ± 4	28 ± 4	≤ 0.5	≤ 0.5			
S114MC-15	1	9.5	0.749	39 ± 7	31 ± 5	≤ 0.8	≤ 0.9			
S114MC-16	1	10.5	0.760	34 ± 7	24 ± 4	≤ 0.8	≤ 0.9			
S114MC-17	1	11.5	0.796	42 ± 8	33 ± 7	≤ 0.9	≤ 1.0			
S114MC-18	1	12.5	0.860	29 ± 4	30 ± 4	≤ 0.4	≤ 0.5			
S114MC-19	1	13.5	0.779	34 ± 4	35 ± 3	≤ 0.5	≤ 0.5			
S114MC-20	1	14.5	0.678	41 ± 4	34 ± 3	≤ 0.4	≤ 0.5			
S114MC-21	2	16	0.616	52 ± 7	38 ± 5	≤ 0.9	≤ 0.9			
S114MC-22	2	18	0.652	59 ± 8	55 ± 6	≤ 1.0	≤ 1.1			
S114MC-23	2	20	0.646	60 ± 8	39 ± 5	≤ 0.9	≤ 1.0			
S114MC-24	2	22	0.726	61 ± 6	43 ± 4	≤ 0.7	≤ 0.7			
S114MC-25	2	24	0.787	53 ± 6	43 ± 4	≤ 0.6	≤ 0.7			
S114MC-26	2	41	0.560	56 ± 8	52 ± 7	≤ 0.9	≤ 1.0			

				Lost Sediment Thickness:
CRS Sedimentation Rate:	0.0074 ± 0.0014 g/cm²/y	^{210}Pb Focus Factor:	0.67	Lost Sediment Dry Bulk Density:
CIC Sedimentation Rate:	0.0091 ± 0.0016 g/cm²/y	^{137}Cs Focus Factor:		Lost Sediment Average Date:

VITA

NAME:	Colin Cook Smalley
EDUCATION:	B.S.Evs., Environmental Science, Creighton University, Omaha, Nebraska, 2010
	M.S., Earth and Environmental Sciences, University of Illinois at Chicago, Chicago, Illinois, 2013
	Graduate Certificate, Geospatial Analysis and Visualization, University of Illinois at Chicago, Chicago, Illinois, 2013
TEACHING EXPERIENCE:	Department of Biology, Creighton University, Omaha, Nebraska: Terrestrial Ecology Laboratory for Undergraduates, 2008 & 2009
	Department of Biology, Creighton University, Omaha, Nebraska: Environmental Science for Undergraduates, 2009
	Department of Atmospheric Science, Creighton University, Omaha, Nebraska: Introduction to Atmospheric Science Laboratory for Undergraduates, 2010
	Department of Earth and Environmental Sciences, University of Illinois at Chicago, Chicago, Illinois: Global Environmental Change Laboratory for Undergraduates, 2011 & 2012
	Department of Earth and Environmental Sciences, University of Illinois at Chicago, Chicago, Illinois: Environmental Geomorphology Laboratory for Undergraduates and Graduate Students, 2012
	Department of Earth and Environmental Sciences, University of Illinois at Chicago, Chicago, Illinois: Earth Systems Laboratory for Undergraduates, 2013
HONORS:	Chancellor's Graduate Research Fellowship, University of Illinois at Chicago, Chicago, Illinois, 2013
	Special Award for Outstanding Achievement in Environmental Science, Creighton University Environmental Science Program, Omaha, Nebraska, 2010

PROFESSIONAL MEMBERSHIP:	Illinois Association for Floodplain and Stormwater Management Association of Environmental and Engineering Geologists Illinois GIS Association
PUBLICATIONS:	Vinton, M.A., Smalley, C.C., Hines, E.M., 2013. The understory tree species, *Ostrya virginiana* (eastern hophornbeam): A "poster child" for shifting forest composition at the prairie-forest boundary in the central United States, Poster accepted for the 98th Annual Meeting of the Ecological Society of America, Minneapolis, MN.